MicroRNA-21 promotes Th17 differentiation and mediates experimental autoimmune encephalomyelitis

Murugaiyan, Gopal ; da Cunha, Andre Pires ; Ajay, Amrendra K ; Joller, Nicole ; Garo, Lucien P ; Kumaradevan, Sowmiya ; Yosef, Nir ; Vaidya, Vishal S ; Weiner, Howard L

Abstract: Accumulation of IL-17–producing Th17 cells is associated with the development of multiple autoimmune diseases; however, the contribution of microRNA (miRNA) pathways to the intrinsic control of Th17 development remains unclear. Here, we demonstrated that miR-21 expression is elevated in Th17 cells and that mice lacking miR-21 have a defect in Th17 differentiation and are resistant to experimental autoimmune encephalomyelitis (EAE). Furthermore, we determined that miR-21 promotes Th17 differentiation by targeting and depleting SMAD-7, a negative regulator of TGF- signaling. Moreover, the decreases in Th17 differentiation in miR-21–deficient T cells were associated with defects in SMAD-2/3 activation and IL-2 suppression. Finally, we found that treatment of WT mice with an anti–miR-21 oligonucleotide reduced the clinical severity of EAE, which was associated with a decrease in Th17 cells. Thus, we have characterized a T cell–intrinsic miRNA pathway that enhances TGF- signaling, limits the autocrine inhibitory effects of IL-2, and thereby promotes Th17 differentiation and autoimmunity.

DOI: https://doi.org/10.1172/JCI74347

MicroRNA-21 promotes Th17 differentiation and mediates experimental autoimmune encephalomyelitis

Gopal Murugaiyan,[1,2] Andre Pires da Cunha,[1,2] Amrendra K. Ajay,[3] Nicole Joller,[1,2,4] Lucien P. Garo,[1,2] Sowmiya Kumaradevan,[1,2] Nir Yosef,[5] Vishal S. Vaidya,[3] and Howard L. Weiner[1,2]

[1]Ann Romney Center for Neurologic Diseases, [2]Evergrande Center for Immunologic Diseases, and [3]Renal Division, Department of Medicine, Brigham and Women's Hospital and Harvard Medical School, Boston, Massachusetts, USA. [4]Institute of Experimental Immunology, University of Zurich, Zurich, Switzerland. [5]Broad Institute of MIT and Harvard, Cambridge, Massachusetts, USA.

Accumulation of IL-17–producing Th17 cells is associated with the development of multiple autoimmune diseases; however, the contribution of microRNA (miRNA) pathways to the intrinsic control of Th17 development remains unclear. Here, we demonstrated that miR-21 expression is elevated in Th17 cells and that mice lacking miR-21 have a defect in Th17 differentiation and are resistant to experimental autoimmune encephalomyelitis (EAE). Furthermore, we determined that miR-21 promotes Th17 differentiation by targeting and depleting SMAD-7, a negative regulator of TGF-β signaling. Moreover, the decreases in Th17 differentiation in miR-21–deficient T cells were associated with defects in SMAD-2/3 activation and IL-2 suppression. Finally, we found that treatment of WT mice with an anti–miR-21 oligonucleotide reduced the clinical severity of EAE, which was associated with a decrease in Th17 cells. Thus, we have characterized a T cell–intrinsic miRNA pathway that enhances TGF-β signaling, limits the autocrine inhibitory effects of IL-2, and thereby promotes Th17 differentiation and autoimmunity.

Introduction

IL-17–producing Th17 cells contribute to protection against microbial pathogens but also play a critical role in the development of autoimmunity (1), including multiple sclerosis (MS) and its animal model experimental autoimmune encephalomyelitis (EAE) (2–5). Multiple cytokines including TGF-β, IL-6, IL-1β, and IL-21 have been shown to induce the differentiation of naive T cells toward the Th17 phenotype (6–11). The differentiation of Th17 cells requires expression of the transcription factor ROR-γt (12). The induction of ROR-γt is dependent on STAT-3, which is preferentially activated by IL-6. In addition, other transcription factors including ROR-α, IRF-4, BATF, and HIF-1α are also involved in the control of Th17 lineage commitment (13–16).

Among the cytokines, TGF-β critically promotes Th17-mediated immune responses. Altered TGF-β and TGF-β receptor (TGF-βR) signaling have been implicated in Th17-mediated autoimmune pathogenesis (6, 7). For example, mice expressing dominant-negative TGF-βRII confer resistance to EAE through a reduction in Th17 cells (17). TGF-β signals are transduced through activation of the SMAD proteins SMAD-2 and SMAD-3 (18), and enhanced generation of Th17 cells is associated with increased TGF-β–induced SMAD-2/3 activation (19–21). In addition, TGF-β signaling has been shown to downregulate IL-2 expression and abrogate IL-2–mediated suppression of Th17 differentiation (20–23). However, the role that microRNAs (miRNAs) play in the activation of TGF-βR signaling in driving Th17 cell development and, consequently, Th17-mediated autoimmunity remains unknown.

miRNAs are a class of small, noncoding RNAs that impart posttranscriptional gene regulation through several mechanisms including translational repression and mRNA degradation (24). They are important in many physiological processes such as carcinogenesis and immune system modulation. Aberrant expression of miRNAs has been linked to a variety of human pathologies including MS and other inflammatory diseases (25, 26).

Here, we report that miR-21 expression was specifically elevated in Th17 cells and that miR-21–deficient (*Mir21*$^{-/-}$) mice showed a defect in Th17 differentiation and strong resistance to EAE. miR-21 promoted Th17 differentiation by targeting SMAD-7, a negative regulator of TGF-β signaling. The defects in Th17 differentiation in *Mir21*$^{-/-}$ T cells were associated with defects in SMAD-2/3 activation and IL-2 suppression. Anti–miR-21 treatment dramatically reduced the clinical severity of EAE and decreased Th17 cell numbers. Thus, our results characterize a previously unknown T cell–intrinsic miRNA pathway that promotes Th17 differentiation and autoimmunity and identifies miR-21 as a potential therapeutic target in the amelioration of MS and other Th17-mediated autoimmune diseases.

Results

miR-21 promotes Th17 differentiation. CD4$^+$ T cells play a major role in autoimmune disease. Increased expression of miR-21 has been observed in human autoimmune conditions including MS, systemic lupus erythematosus (SLE), and psoriasis (27–30). However, the role of miR-21 and its intrinsic requirement in Th cell differentiation and autoimmunity remains unclear. To investigate the expression of miR-21 in Th cell subsets, we activated naive CD4$^+$CD62L^{hi}CD44^{lo} T cells under polarizing conditions in vitro and obtained Th1, Th2, Th17, and Treg cells with selective expression of *Ifng*, *Il4*, *Il17*, and *Foxp3*, respectively (Supplemental Figure 1A; supplemental material available online with this

Conflict of interest: The authors have declared that no conflict of interest exists.
Submitted: November 19, 2013; **Accepted:** December 16, 2014.
Reference information: *J Clin Invest.* doi:10.1172/JCI74347.

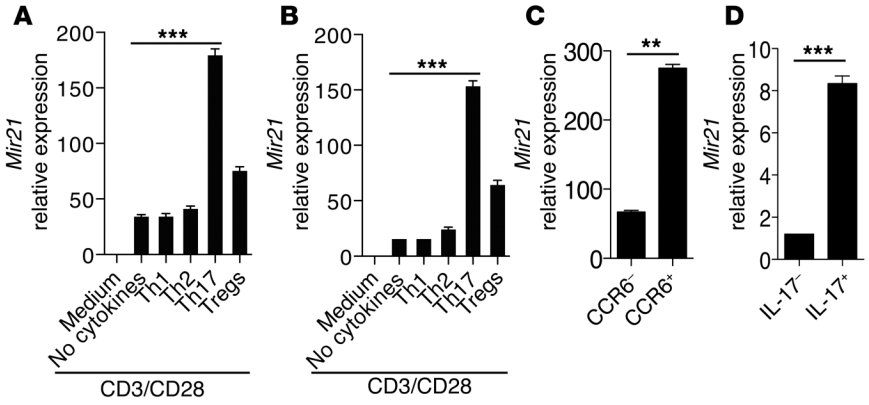

Figure 1. miR-21 is specifically induced in Th17 cells. (**A** and **B**) Naive $CD4^+CD62L^{hi}CD44^{lo}$ T cells were activated with plate-bound anti-CD3 (2 μg/ml) and anti-CD28 (2 μg/ml) in the presence of Th1-, Th2-, Th17-, and Treg-polarizing conditions in vitro. Twenty-four hours later, miR-21 expression was analyzed by quantitative RT-PCR (qRT-PCR) using the snRNAs snoRNA135 and U6 snRNA as endogenous controls. (**C**) qRT-PCR analysis of miR-21 expression in flow cytometric–sorted $CCR6^+CD4^+$ and $CCR6^-CD4^+$ T cells from in vitro Th17 cultures. (**D**) $CD4^+$ T cells from C57BL/6 mice were sorted into $IL\text{-}17A^+$ and $IL\text{-}17A^-$ cell populations and analyzed for expression of miR-21 by qRT-PCR. Data are representative of 3 independent experiments. Error bars represent the mean ± SEM. $^{**}P < 0.01$ and $^{***}P < 0.001$ by unpaired Student's *t* test. Med, medium.

article; doi:10.1172/JCI74347DS1). We found large amounts of miR-21 in Th17 cells and relatively small amounts in Th1, Th2, and inducible Tregs (iTregs) (Figure 1, A and B). We used 2 different endogenous controls (small nucleolar RNA135 [snoRNA135] and U6 small nuclear RNA [snRNA]) to analyze miR-21 expression in T cells and found similar results (Figure 1, A and B). We then investigated whether T cell antigen receptor (TCR) stimulation was required for TGF-β and IL-6–induced miR-21 upregulation in T cells and found that stimulation via the TCR and CD28 led to a small increase in miR-21 levels compared with that observed in unstimulated cells. The addition of TGF-β and IL-6 further increased miR-21 expression (Supplemental Figure 1B). Moreover, miR-21 was specifically upregulated in T cells that were stimulated under Th17 conditions (Figure 1, A and B).

Th17 cells have been reported to express chemokine receptor CCR6 (31). To test whether IL-17 expression in $CCR6^+$ cells correlated with miR-21 expression, we sorted $CCR6^+$ and $CCR6^-$ T cells from Th17 cultures and found that $CCR6^+$ cells had higher miR-21 expression than did $CCR6^-$ cells (Figure 1C), along with increased *Il17* expression (Supplemental Figure 1C). Although in vitro polarization recapitulates the phenotypes of different Th lineages, in vitro and in vivo polarized cells may not be identical. Therefore, we assessed miR-21 expression levels in freshly isolated T cells. To this end, $CD4^+$ T cells were sorted ex vivo based on IL-17 expression as assessed using an IL-17 secretion assay. Consistent with the data obtained from in vitro polarized cells, IL-17–secreting cells expressed higher levels of miR-21 when compared with the levels seen in $IL\text{-}17^-CD4^+$ T cells (Figure 1D), along with the enrichment of IL-17 expression (Supplemental Figure 1D). Taken together, these data indicate that miR-21 is differentially expressed in Th17 cells.

To directly assess whether miR-21 regulated the differentiation of Th17 cells, we performed an in vitro T cell differentiation assay. When naive $CD4^+$ T cells were activated under Th17-polarizing conditions, IL-17 production in *Mir21*$^{-/-}$ T cells was significantly reduced compared with that in WT T cells (Figure 2, A and B). Consistent with this, *Mir21*$^{-/-}$ T cells differentiated under Th17-polarizing conditions expressed lower levels of Th17-associated transcription factors (*Rorgt*, *Rora*, *Irf4*, *Hif1a*, and *Batf*), cytokines (*Il17f*, *Il21*, *Il22*, and *Gmcsf*), and cell-surface receptors (*Il23r* and *Ccr6*) (Figure 2, C–E). In contrast, in vitro differentiation of Th1 and Th2 effector cells was largely independent of miR-21 (Supplemental Figure 2A). Phenotypical analysis of iTregs revealed a dispensable role of miR-21 in iTreg cell differentiation, as reflected by unaltered FOXP3 expression (Supplemental Figure 2B). Moreover, we detected no developmental defect in the generation of $CD25^+FOXP3^+$ natural Tregs (nTregs) in the absence of miR-21 (Supplemental Figure 2C). To investigate whether deletion of miR-21 affected the homeostasis of T cells, B cells, and DC populations, we analyzed 6- to 8-week-old naive *Mir21*$^{-/-}$ mice and WT control mice. In the thymus, the frequencies of $CD4^+$ and $CD8^+$ single-positive as well as $CD4^+CD8^+$ double-positive T cells were unaltered (Supplemental Figure 3A). In addition, we found comparable sizes of lymphoid and myeloid cell subsets in the spleen (Supplemental Figure 3, A–D). Furthermore, the size and total cellularity of spleens and inguinal lymph nodes (LNs) were comparable between WT and *Mir21*$^{-/-}$ mice (Supplemental Figure 3, E and F). Collectively, these results provide evidence that miR-21 is not required to effectively induce Th1, Th2, or Tregs and suggest a selective role for miR-21 in Th17 cells.

miR-21 regulates EAE development. These observations led us to explore the potential role of miR-21 in Th17-mediated inflammatory immune pathogenesis in vivo. To investigate the role of miR-21 in EAE development, we first analyzed the expression of miR-21 in mice during the course of EAE. Since $CD4^+$ T cells are the key mediators of EAE, we asked whether $CD4^+$ T cells express miR-21 during EAE. We analyzed miR-21 expression in $CD4^+$T cells from C57BL/6 mice immunized against EAE with $MOG_{35–55}$ peptide emulsified in CFA and found that miR-21 expression was markedly increased in $CD4^+$ T cells isolated from the spleen and CNS of EAE mice compared with that in naive mice (Figure 3A). The potential role of miR-21 in EAE pathogenesis was then tested using *Mir21*$^{-/-}$ mice. In 4 independent experiments, *Mir21*$^{-/-}$ mice were resistant to EAE induction (2 of 38 mice developed EAE), whereas WT mice developed severe EAE (35 of 38 mice developed EAE) (Figure 3B). The absence of paralytic symptoms in *Mir21*$^{-/-}$ mice was associated with a marked reduction in inflammation and demyelination (Figure 3, C and D). Although we found that EAE was associated with demyelination and infiltration of $CD4^+$ T cells and $CD11c^+$ cells from the peripheral lymphoid organs to the CNS in both WT and *Mir21*$^{-/-}$ mice, the total number of $CD4^+$ T cells and $CD11c^+$ cells was markedly lower in the CNS of *Mir21*$^{-/-}$ mice at the peak of disease (Figure 3E).

miR-21 has been reported to target various tumor-suppressor genes such as *Btg2*, *Pdcd4*, *Pten*, and sprouty, which are known to regulate cell death and proliferation (32–39). We therefore tested

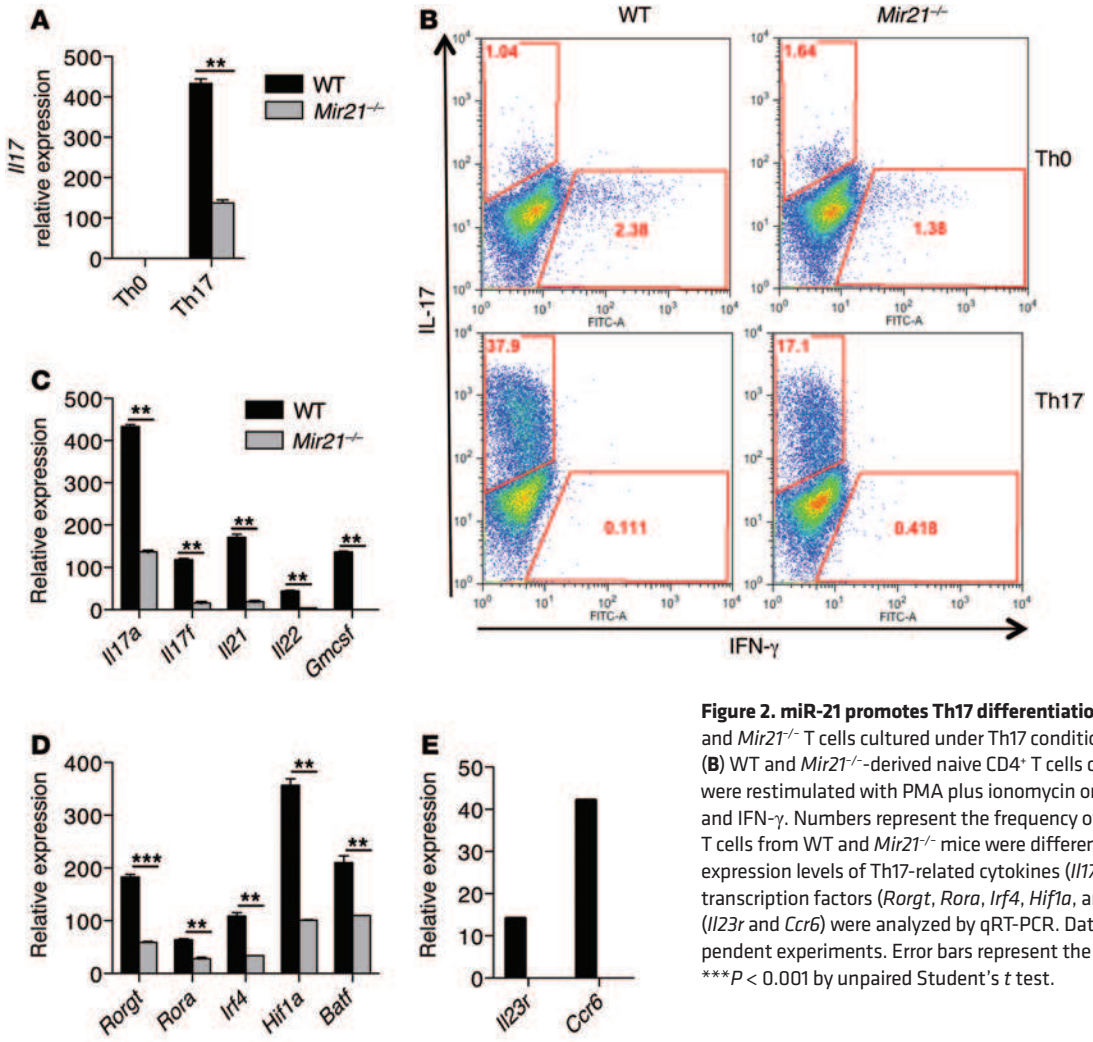

Figure 2. miR-21 promotes Th17 differentiation. (**A**) *Il17a* expression in WT and *Mir21*$^{-/-}$ T cells cultured under Th17 conditions determined by qRT-PCR. (**B**) WT and *Mir21*$^{-/-}$-derived naive CD4$^+$ T cells cultured under Th17 conditions were restimulated with PMA plus ionomycin on day 5 and stained for IL-17 and IFN-γ. Numbers represent the frequency of CD4$^+$ T cells. (**C**–**E**) Naive CD4$^+$ T cells from WT and *Mir21*$^{-/-}$ mice were differentiated into Th17 cells. mRNA expression levels of Th17-related cytokines (*Il17a*, *Il17f*, *Il21*, *Il22*, and *Gmcsf*), transcription factors (*Rorgt*, *Rora*, *Irf4*, *Hif1a*, and *Batf*), and surface receptors (*Il23r* and *Ccr6*) were analyzed by qRT-PCR. Data are representative of 3 independent experiments. Error bars represent the mean ± SEM. $^{**}P < 0.01$, and $^{***}P < 0.001$ by unpaired Student's *t* test.

whether miR-21 affects the cell death and proliferation of CD4$^+$ T cells by targeting these tumor suppressors. Although we found that in vitro–stimulated *Mir21*$^{-/-}$ T cells expressed higher levels of *Pten* than did their WT counterparts (Supplemental Figure 4A), no significant differences in the expression of these target genes were observed between WT and *Mir21*$^{-/-}$ T cells in vivo (Supplemental Figure 4B). Consistent with the increased expression of *Pten* in vitro, we found that naive *Mir21*$^{-/-}$ T cells stimulated in vitro exhibited a proliferative defect (Supplemental Figure 4C). However, we found no significant differences in any of the examined proliferative parameters between MOG-immunized WT and *Mir21*$^{-/-}$ T cells in response to MOG antigen (Supplemental Figure 4D). In addition, no difference in the frequencies of apoptotic T cells between WT and *Mir21*$^{-/-}$ mice was observed (Supplemental Figure 4, E and F) either in vitro or in vivo. Consistent with these findings, the total spleen cellularity, frequency of activated (CD44^{hi}) CD4$^+$ T cells, and percentage of MOG-tetramer$^+$ T cells were similar between WT and *Mir21*$^{-/-}$ mice during EAE induction (Supplemental Figure 4, G–I). Together, these results establish the presence of MOG-specific T cells in *Mir21*$^{-/-}$ mice and demonstrate the ability of these T cells to expand in response to MOG peptide, suggesting that a general proliferative or apoptotic abnormality in *Mir21*$^{-/-}$ T cells is not a major contributor to the striking EAE resistance we observed in these mice.

We further investigated whether the EAE resistance in *Mir21*$^{-/-}$ was associated with a defect in cytokine production from T cells. At peak disease, CNS-infiltrating CD4$^+$ T cells from *Mir21*$^{-/-}$ mice produced less IL-17, whereas IFN-γ levels were unaffected (Figure 3F). In line with a reduction in the frequency of IL-17–producing cells in the CNS, mRNA expression of other Th17-associated genes in T cells from *Mir21*$^{-/-}$ mice was also reduced in comparison with expression in T cells from WT mice (Figure 3G). Consistent with these RNA data, analysis of CNS-infiltrating Th17 cells for intracellular cytokines revealed a significant defect in expression of the Th17-related cytokines IL-17A and IL-17F in *Mir21*$^{-/-}$ mice. However, the protein levels of IL-21 and IL-22 were not altered between WT and *Mir21*$^{-/-}$ mice (Supplemental Figure 5). In addition, we found that *Mir21*$^{-/-}$ mice had substantially reduced percentages (Figure 3H) and absolute numbers (Supplemental Figure 6) of Th17 cells in the CNS compared with those detected in WT mice at the onset and peak stages of EAE. Furthermore, we found that *Mir21*$^{-/-}$ mice had substantially diminished percentages of Th17 cells in the periphery compared with those detected in WT mice at the onset and peak stages of EAE (Supplemental Figure 7).

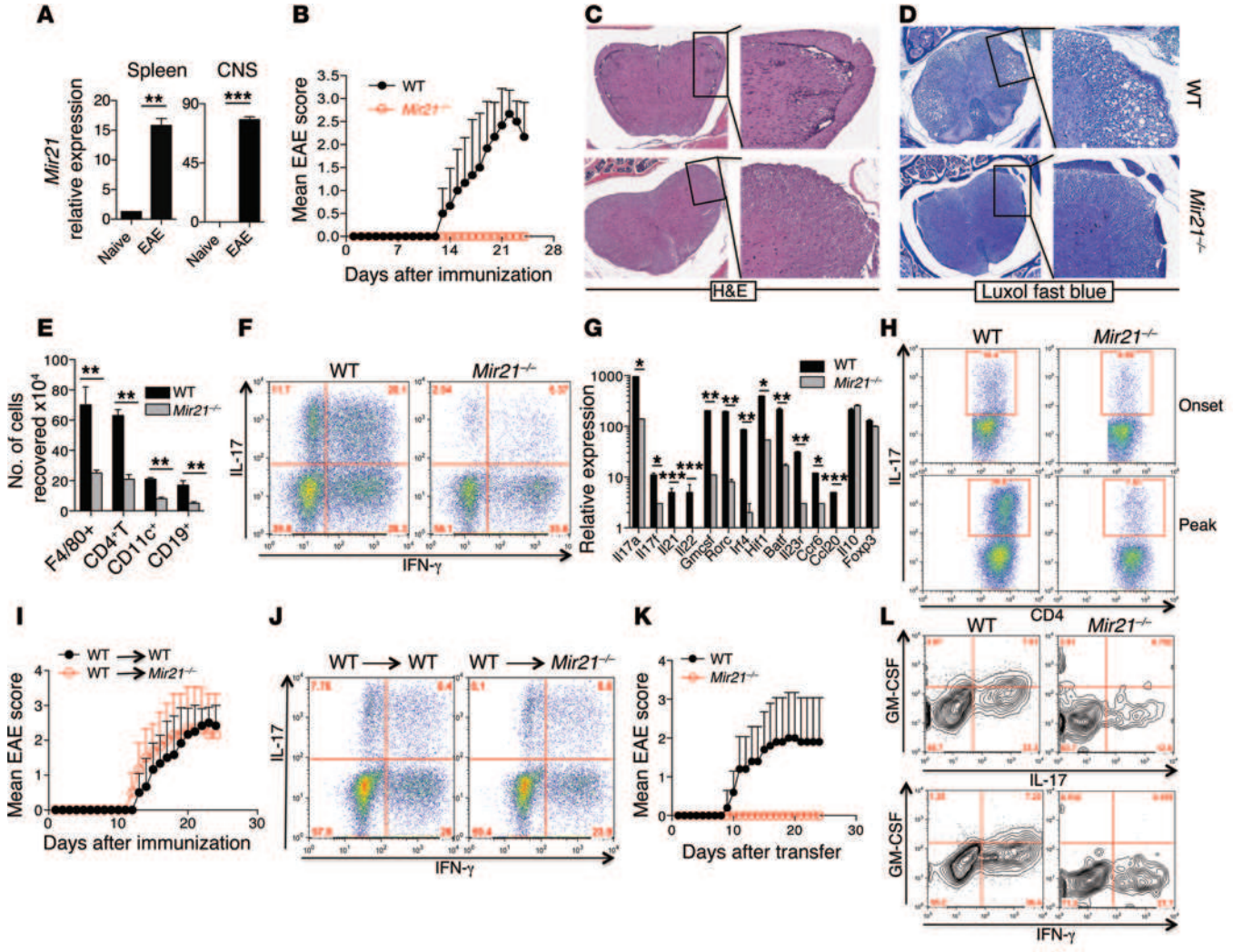

Figure 3. miR-21–deficient mice are resistant to EAE. (**A**) *Mir21* mRNA was determined by RT-PCR analysis in CD4$^+$ T cells from the spleen and then the CNS of naive and EAE mice at peak disease stage. (**B**) Clinical scores of WT and *Mir21*$^{-/-}$ mice (n = 8) after immunization with $MOG_{33–55}$ in CFA. (**C** and **D**) Histopathological analysis of spinal cord sections from WT and *Mir21*$^{-/-}$ mice (n = 3) 20 days after immunization. Original magnification, ×20 (**C**) and ×40 (**D**). (**E**) Mononuclear cell numbers pooled from the CNS of WT and *Mir21*$^{-/-}$ mice (n = 3) 20 days after immunization. (**F**) Intracellular staining of IFN-γ and IL-17 in CNS-derived CD4$^+$ T cells from WT and *Mir21*$^{-/-}$ mice with EAE. Numbers indicate the percentage of CD4$^+$ cells. (**G**) mRNA expression of Th17-related cytokines, transcription factors, and surface receptors from CD4$^+$ T cells within the CNS as determined by RT-PCR. (**H**) FACS analysis of frequencies of IL-17–producing CD4$^+$ T cells from the CNS of the indicated groups. (**I**) WT and *Mir21*$^{-/-}$ mice (n = 5) were injected i.v. with WT CD4$^+$ T cells 5 days before EAE induction. (**J**) FACS analysis of frequencies of IFN-γ– and IL-17–producing CD4$^+$ T cells from the CNS of the indicated groups. (**K**) Disease course of adoptive EAE in WT recipients, reconstituted with Th17-polarized cells from WT or *Mir21*$^{-/-}$ mice (n = 5). (**L**) FACS analysis of frequencies of GM-CSF–, IL-17–, and IFN-γ–producing CD4$^+$ T cells from the CNS of the indicated groups. Data are representative of 3 independent experiments. Error bars represent the mean ± SEM. *P < 0.05, **P < 0.01, and ***P < 0.001 by unpaired Student's t test.

Together, these data demonstrate that miR-21 positively regulates Th17 differentiation both in vivo and in vitro.

DCs play an important role in the development of EAE and produce inflammatory cytokines that are required for Th17 differentiation and function in vivo (8). Among the DC-secreted cytokines, IL-23 is crucial for the functional maturation of Th17 cells. In fact, IL-23R–deficient mice were shown to be resistant to EAE, owing to a specific defect in Th17 cells (40). To investigate the possibility that impaired Th17 differentiation in *Mir21*$^{-/-}$ mice was caused by a defect in DCs, we evaluated inflammatory cytokine expression and costimulatory molecule expression in DCs. We found that DCs from both WT and *Mir21*$^{-/-}$ mice expressed normal levels of costimulatory molecules (Supplemental Figure 8A) and Th17-polarizing cytokines *Il6*, *Il23*, *Il1b*, and *Tnfa* after LPS stimulation (Supplemental Figure 8B). In addition, coculture of naive CD4$^+$ T cells and DCs indicated that *Mir21*$^{-/-}$ DCs were able to support Th17 development normally. However, Th17 development from *Mir21*$^{-/-}$ naive CD4$^+$ T cells was markedly impaired, regardless of the origin of the cocultured DCs (Supplemental Figure 8C). IL-17–producing innate lymphoid cells have been shown to play a pathological role in certain autoimmune diseases (41). However, we did not find any difference between WT and *Mir21*$^{-/-}$ mice in the frequency of innate lymphoid cells or the expression of IL-17 in these cells (Supplemental Figure 9). Collectively, these data

suggest that *Mir21*$^{-/-}$ CD4$^+$ T cells have an intrinsic defect in their ability to differentiate into Th17 cells, resulting in amelioration of EAE in *Mir21*$^{-/-}$ animals.

To establish that the resistance to EAE in *Mir21*$^{-/-}$ mice resulted from a T cell–intrinsic defect, we transferred WT CD4$^+$ T cells into WT or *Mir21*$^{-/-}$ mice before MOG immunization. Both WT and *Mir21*$^{-/-}$ mice receiving CD4$^+$ T cells from WT mice developed EAE accompanied by CNS-infiltrating IL-17–producing CD4$^+$ T cells, suggesting that miR-21–sufficient T cells from WT mice can overcome the EAE resistance in *Mir21*$^{-/-}$ mice (Figure 3, I and J). We further examined whether the EAE resistance of *Mir21*$^{-/-}$ mice might be due to their nonfunctional T cells. To test this hypothesis, MOG-specific Th17 and Th1 cells of *Mir21*$^{-/-}$ and WT origin were injected into syngeneic WT recipients, and the animals were monitored for signs of EAE. While the recipients of Th17 cells from WT mice developed severe EAE, Th17 cells from *Mir21*$^{-/-}$ mice were not able to induce disease (Figure 3K). Interestingly, we found that injection of MOG-specific WT Th1 cells resulted in severe EAE, whereas, transfer of MOG-specific *Mir21*$^{-/-}$ Th1 cells did not elicit any signs of EAE (Supplemental Figure 10). GM-CSF is the main effector cytokine in both Th1 and Th17 cell–driven EAE (42–44). In fact, Th1 cells that lack the ability to produce GM-CSF do not transfer EAE (42). We therefore assessed GM-CSF expression in Th1 and Th17 cells infiltrating the brains of WT and *Mir21*$^{-/-}$ mice with EAE. Interestingly, CNS-infiltrating Th1 and Th17 cells from *Mir21*$^{-/-}$ mice showed a dramatic drop in GM-CSF expression, suggesting that miR-21 is critical for the encephalitogenic function of T cells in vivo (Figure 3L). It has been shown that the recruitment of myeloid cells is associated with pathogenic Th17 responses and GM-CSF secretion (45). Consistent with our observation of impaired IL-17 and GM-CSF secretion by CNS-infiltrating *Mir21*$^{-/-}$ Th17 cells, we observed a significant reduction in the number of CNS-infiltrating DCs and macrophages in *Mir21*$^{-/-}$ mice (Figure 3E). It has also been shown that Th17 cells initially access the CNS and create a microenvironment conducive to the subsequent entry of Th1 cells (31). The defective Th17 differentiation, coupled with a reduction of GM-CSF secretion by both Th1 and Th17 cells, could explain the highly resistant EAE phenotype observed in *Mir21*$^{-/-}$ mice. Together, these observations demonstrate that EAE resistance in *Mir21*$^{-/-}$ mice is caused by T cell–intrinsic defects.

miR-21 promotes Th17 differentiation through SMAD-7 inhibition. We then investigated the mechanism by which miR-21 regulates Th17 development. It is possible that miR-21 could control Th17 development by regulating IL-6 and TGF-β signaling. A critical mechanism of Th17 differentiation is IL-6–induced STAT-3 activation (46). However, we did not find any difference in phosphorylated STAT-3 (p–STAT-3) levels between WT and *Mir21*$^{-/-}$ CD4$^+$ T cells stimulated with IL-6 (Supplemental Figure 11A). In addition, there was no difference in IL-6 receptor (IL-6R) expression between the 2 genotypes, suggesting that *Mir21*$^{-/-}$ does not play a role in the modulation of signaling events downstream of the IL-6R (Supplemental Figure 11B). TGF-β initiates its cellular function by binding to TGF-βRII, which then phosphorylates TGF-βRI. TGF-βRI propagates the signal by inducing SMAD-2 and SMAD-3 phosphorylation, which subsequently leads to nuclear translocation, SMAD-2 and SMAD-3 DNA binding, and the transcriptional activation of TGF-β–responsive genes (18). Although we did not find any defect in TGF-β or TGF-βR expression in *Mir21*$^{-/-}$ CD4$^+$ T cells (Supplemental Figure 12), stimulation of *Mir21*$^{-/-}$ CD4$^+$ T cells with TGF-β resulted in reduced phosphorylation of both SMAD-2 and SMAD-3 when compared with that in WT CD4$^+$ T cells (Figure 4A). Strikingly, stimulation of *Mir21*$^{-/-}$ CD4$^+$ T cells with TGF-β resulted in higher SMAD-7 expression (Figure 4B). Contrary to the function of SMAD-2/3, TGF-β–induced SMAD-7 participates in a negative feedback loop to control excessive TGF-β signaling.

We thus applied the Web-based target prediction software program TargetScan (www.targetscan.org) to identify potential miR-21 targets and found miR-21 to be a potential upstream regulator of SMAD-7 (Figure 4C). In addition, recent data from other disease models suggest that miR-21 is an upstream regulator of SMAD-7 (47, 48). To determine whether SMAD-7 is a target of miR-21 in Th17 differentiation, we performed luciferase assays using the WT and mutant *Smad7* 3′ UTR. We found that miR-21 inhibited the luciferase activity of a reporter containing the WT *Smad7* 3′ UTR, but not that of a reporter with a mutated 3′ UTR unable to bind to miR-21 (Figure 4, D and E). The effect of miR-21 on SMAD-7 expression was then tested by using a chemically modified locked nucleic acid (LNA) inhibitor. We found that inhibition of miR-21 led to an increase in SMAD-7 expression in CD4$^+$ T cells treated with TGF-β (Figure 4F). Consistent with the increased levels of SMAD-7, inhibition of miR-21 also led to decreased phosphorylation of SMAD-2 and SMAD-3 in CD4$^+$ T cells (Figure 4F). On the other hand, miR-21 overexpression substantially decreased the levels of SMAD-7 while increasing the expression of SMAD-2 and SMAD-3 (Figure 4G). In addition to the SMAD-dependent signaling pathway, TGF-β is also known to signal via a SMAD-independent pathway (18). However, we did not find any difference between WT and *Mir21*$^{-/-}$ T cells in the activation levels of molecules associated with non-SMAD TGF-β signaling pathways including p38 MAPK, ERK-1/2, and stress-activated protein kinase (SAPK)/Jun amino-terminal kinase (JNK) (Supplemental Figure 13). Taken together, our results suggest that by targeting SMAD-7, miR-21 promotes SMAD-mediated TGF-β signaling and that its deletion results in reduced sensitivity to the effects of TGF-β in T cells.

Next, we tested the functional role of miR-21 in regulating the effects of TGF-β on Th17 differentiation and the role of SMAD-7 in regulating these effects. CD4$^+$ T cells were transfected with lentiviral shRNA against SMAD-7 and cultured under Th17 conditions. Knockdown of SMAD-7 in CD4$^+$T cells resulted in increased production of IL-17 and other Th17-related cytokines with concomitant downregulation of IL-2 (Figure 4, H–J). Consistent with the downregulation of IL-2, SMAD-7 inhibition resulted in enhanced SMAD-2 and SMAD-3 phosphorylation (Figure 4K). Similarly, we found an increase in IL-17 levels when SMAD-7 was knocked down in CD4$^+$ T cells using SMAD-7–conditional–KO mice (Figure 4L). To determine whether reducing SMAD-7 levels in *Mir21*$^{-/-}$ mice would restore Th17 differentiation in *Mir21*$^{-/-}$ CD4$^+$ T cells, we blocked SMAD-7 expression using lentiviral shRNAs and found that blocking SMAD-7 activity restored IL-17 levels in *Mir21*$^{-/-}$ Th17 cells, which was associated with a reduction in IL-2 levels (Figure 4M). It has been demonstrated that TGF-β inhibits IL-2 production of T cells in a SMAD-3–dependent manner (22, 47). In addition, a SMAD-binding element

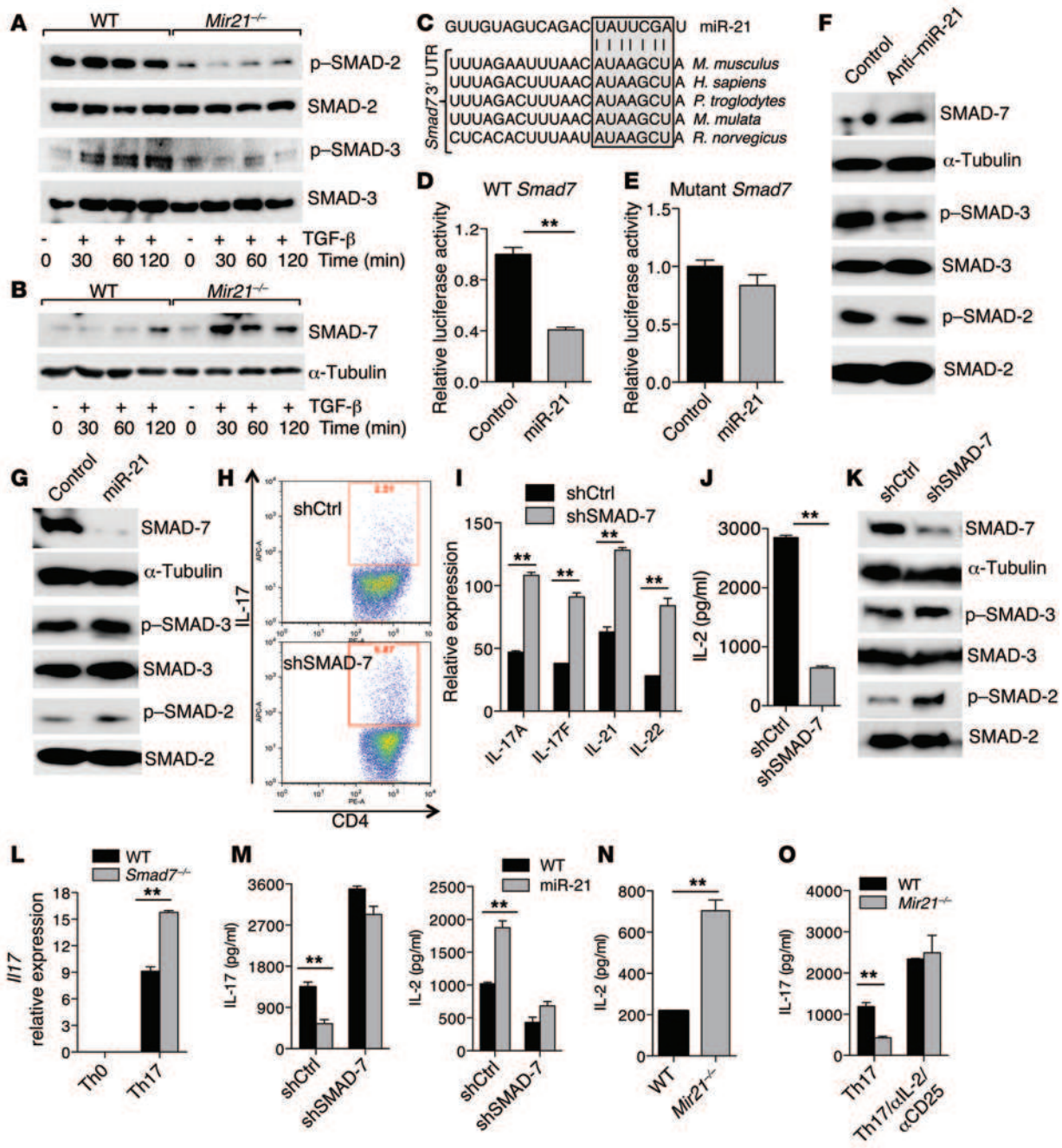

Figure 4. miR-21 promotes Th17 differentiation by targeting SMAD-7. (**A** and **B**) Representative immunoblots of phosphorylated and total SMAD-2/3/7 proteins in CD4$^+$ T cells from WT and *Mir21*$^{-/-}$ mice stimulated with TGF-β (2 ng/ml) for the indicated times. (**C**) miR-21 aligned with the highly conserved 3′ UTR of *Smad7* mRNA. (**D** and **E**) Luciferase activity of a reporter carrying a mutant or WT *Smad7* 3′ UTR cotransfected into HEK-293 T cells with miR-21 or with its control. (**F**) Western blot analysis of SMAD-7, p–SMAD-2, and p–SMAD-3 in CD4$^+$ T cells from WT mice treated with miR-21 inhibitors or with its control. (**G**) Western blot analysis of SMAD-7, p–SMAD-2, and p–SMAD-3 in CD4$^+$ T cells from WT mice treated with miR-21 precursors or with its control. (**H** and **I**) SMAD-7 knockdown increased IL-17 and expression of other Th17-related cytokines in CD4$^+$ T cells. Numbers represent the frequency of CD4$^+$ cells. (**J**) ELISA of IL-2 in Th17 cells transduced with control or SMAD-7–specific shRNA. (**K**) SMAD-7 knockdown increased TGF-β–induced SMAD-2/3 phosphorylation, while downregulating SMAD-7 levels. (**L**) *Il17* expression in WT and *Smad7*$^{-/-}$ T cells cultured under Th17 conditions. (**M**) SMAD-7 knockdown increased IL-17, while downregulating IL-2 in *Mir21*$^{-/-}$ Th17 cells. (**N**) ELISA of IL-2 in Th17 cells from WT and *Mir21*$^{-/-}$ mice. (**O**) Neutralization of IL-2 restored IL-17 levels in *Mir21*$^{-/-}$ Th17 cells. Data are representative of 2 to 3 independent experiments. Error bars represent the mean ± SEM. $^{**}P < 0.01$ and $^{***}P < 0.001$ by unpaired Student's *t* test.

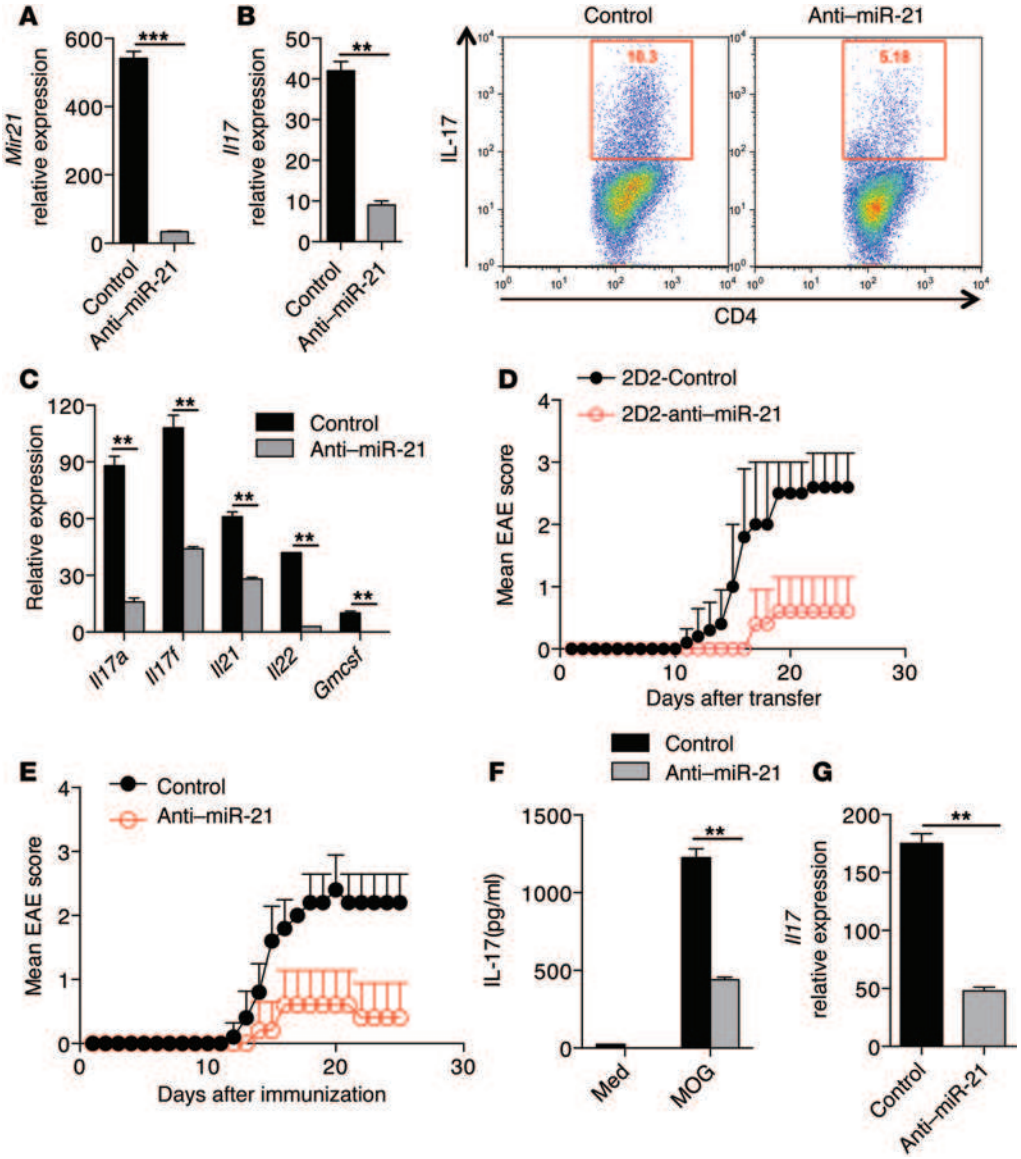

Figure 5. Silencing miR-21 ameliorates the clinical severity of EAE. (**A**) qRT-PCR analysis of miR-21 in naive CD4$^+$ T cells cultured for 24 hours under Th0 conditions and transfected by nucleofection with the miR inhibitor LNA–anti–miR-21 or scrambled control antisense oligonucleotide (LNA control), followed by Th17 differentiation for another 24 hours. (**B**) qRT-PCR and flow cytometric analysis of IL-17 in naive CD4$^+$ T cells cultured for 24 hours in Th0 conditions and transfected by nucleofection with the miRNA inhibitor LNA–anti–miR-21 or scrambled control antisense oligonucleotide (LNA control), followed by Th17 differentiation for another 4 days. Numbers represent the frequencies of CD4$^+$ T cells. (**C**) qRT-PCR analysis of Th17-related cytokines in Th17 cells polarized in the presence of control and anti–miR-21 inhibitors. (**D**) Disease course of adoptive EAE in WT recipients (n = 6), reconstituted with Th17 cells polarized in the presence of control and miR-21 inhibitors. (**E**) Silencing miR-21 ameliorated the clinical severity of EAE. Clinical EAE scores for WT mice (n = 6) treated with anti–miR-21 or scrambled control on days 5, 7, 9, 11, and 13 after immunization. (**F**) Splenocytes obtained from anti–miR-21 and scrambled control–treated mice were restimulated with $MOG_{35–55}$ (20 μg/ml) for 72 hours. Cell-free supernatants were assayed for IL-17 by ELISA. (**G**) qRT-PCR analysis of *Il17* in CNS-derived CD4$^+$ T cells isolated from mice treated with or without anti–miR-21. Results are representative of 2 independent experiments. Error bars represent the mean ± SEM. $^{**}P < 0.01$ and $^{***}P < 0.001$ by unpaired Student's t test.

(SBE) is located upstream of the *Il2* promoter, which is important for SMAD-mediated transcriptional suppression of IL-2 (49, 50). Furthermore, IL-2 has been shown to inhibit Th17 differentiation both in vitro and in vivo (23, 51, 52). In order to elucidate the connection between impaired TGF-β–mediated SMAD signaling and reduced Th17 responses in the absence of miR-21, we investigated IL-2 expression. Substantially elevated levels of IL-2 were observed in Th17 cells from *Mir21*$^{-/-}$ T cells compared with the levels detected in Th17 cells from WT T cells, which correlated with less production of IL-17 by *Mir21*$^{-/-}$ T cells (Figure 4N). To determine whether the increased production of IL-2 in *Mir21*$^{-/-}$ mice inhibited the generation of Th17 cells, we blocked IL-2 activity in Th17 cultures using a combination of neutralizing anti–IL-2 and blocking anti–CD25 antibodies and found that blocking IL-2 activity restored IL-17 levels in *Mir21*$^{-/-}$Th17 cells (Figure 4O). Together, these observations demonstrate that miR-21 limits the production of IL-2 to promote Th17 differentiation. Furthermore, enhanced IL-2 levels can offset the effect of TGF-β in *Mir21*$^{-/-}$ T cells and might explain the normal differentiation of Tregs observed in these mice.

Silencing miR-21 ameliorates the clinical severity of EAE. The effect of miR-21 on IL-17 expression was then tested using the miRNA inhibitor LNA–anti–miR-21. We found that silencing miR-21 in vitro led to decreased levels of miR-21 and *Il17* transcripts in T cells cultured under Th17-polarizing conditions (Figure 5, A and B). Furthermore, miR-21 silencing significantly decreased the expression of other cytokines that are related to the Th17 phenotype (Figure 5C). We next investigated whether silencing miR-21 could inhibit the encephalitogenicity of Th17 cells in vivo. For this, we stimulated MOG-specific 2D2 T cells under Th17-polarizing conditions in the presence of control or anti–miR-21 inhibitors and transferred the resulting T cells into syngeneic WT mice. Transplanted mice were injected with pertussis toxin (PT) on the day of T cell transfer and 48 hours later and monitored for the development of EAE. We found that mice that received Th17 cells differentiated in the presence of control

inhibitor developed EAE. However, anti–miR-21 treatment suppressed EAE induced by adoptive transfer of T cells differentiated under Th17-polarizing conditions (Figure 5D). We and others have demonstrated the therapeutic efficacy of LNA-modified oligonucleotide (LNA–anti-miR-21) in EAE and other disease models (53–55). We therefore investigated whether systemic administration of anti–miR-21 in vivo affects the course of EAE. Administration of LNA-modified anti–miR-21 during the preclinical stage of EAE (beginning on day 5 after immunization) substantially ameliorated clinical disease (Figure 5E). To investigate whether anti–miR-21 treatment affected Ag-specific IL-17 recall responses, we isolated spleens from MOG-immunized mice treated with scrambled control or anti–miR-21 and stimulated them in vitro with MOG peptide. We found that splenocytes from anti–miR-21–treated mice had diminished MOG-specific IL-17 expression (Figure 5F). In addition, consistent with our data and with the inhibitory effect of anti–miR-21 on clinical EAE symptoms, we found that anti–miR-21 treatment prevented upregulation of *Il17* transcripts in $CD4^+$ T cells isolated from the CNS of anti–miR-21–treated mice (Figure 5G).

Discussion

Th17 cells play an important role in inflammation and autoimmunity. Although the differentiation of Th17 cells is known to be regulated by specific transcription factors and cytokines, the role of miRNA pathways that intrinsically control Th17 differentiation remains elusive. Here, we report that miR-21 expression is specifically elevated in Th17 cells. $CD4^+$ T cells lacking miR-21 exhibit a specific Th17 cell defect in vitro and during neuroinflammatory disease in vivo. Resistance to EAE induction in *Mir21*$^{-/-}$ mice and the substantial reduction of IL-17^+ CNS cell infiltrates in these mice demonstrate that miR-21 is crucial for the control of Th17 development. Critically, we found that in vivo silencing of miR-21 using LNA-modified anti–miR-21 reduced the clinical severity of EAE and was associated with a decrease in Th17 cells.

TGF-β signaling plays an essential role in the generation of Th17 cells (6–8), yet little is known about the miRNA pathways that intrinsically control these pathways. Our results suggest that miR-21 promotes Th17 differentiation by targeting SMAD-7, a negative regulator of TGF-β signaling. SMAD-7 inhibits TGF-β–induced transcriptional responses by blocking activation of SMAD-2/3 and their complex formation with SMAD-4 (18). Most importantly, SMAD-7 has been shown to bind to SMAD-2 and SMAD-3, which are thought to competitively bind to TGF-βRI, and prevents their activation upon TGF-β stimulation. Mechanistically, we have shown that miR-21 deficiency renders T cells less sensitive to TGF-β–induced SMAD-2/3 activation due to enhanced SMAD-7. Overexpression of miR-21 reduced SMAD-7 expression while upregulating SMAD-2/3 levels, and miR-21 knockdown reversed this TGF-β–induced SMAD-7 expression. Furthermore, silencing SMAD-7 resulted in enhanced IL-17 production, which correlated with increased SMAD-2/3 activation in T cells. Consistent with our data, a recent study demonstrated that the generation of Th17 cells is associated with increased TGF-β–induced SMAD-2/3 activation (21). As a functional miR-21 target, SMAD-7 therefore represents a distinct regulator of Th17 differentiation.

TGF-β signaling through SMAD-dependent and SMAD-independent pathways plays a role in Treg differentiation and function (56–61). Although TGF-β signaling through the SMAD-2/3 pathway has been demonstrated to partially regulate iTreg differentiation, it has also been shown that a combination of SMAD-2 and SMAD-3 deficiency does not alter FOXP3 expression or the suppressive activity of iTregs in vivo (58). In fact, the development, homeostasis, and function of Tregs remained intact in SMAD-2 and SMAD-3 double–deficient mice, suggesting a role for a SMAD-independent pathway in Treg differentiation and function (60). Among the SMAD-independent TGF-β signaling pathways, p38 MAPK signaling has been shown to be required for the conversion of naive $CD4^+$T cells into iTregs (61). Furthermore, IL-2 has been shown to stabilize TGF-β–induced FOXP3 expression and compensate for the loss of defective SMAD-dependent TGF-β signaling in iTreg differentiation (21). Our observation of enhanced IL-2 levels and the unaltered SMAD-independent TGF-β signaling pathway in *Mir21*$^{-/-}$ T cells seems to be able to offset the effect of TGF-β in these cells and might explain the normal differentiation of Tregs observed in *Mir21*$^{-/-}$ mice.

IL-2 has been shown to negatively regulate Th17 differentiation both in vitro and in vivo (23, 49, 52, 62). For example, the uptake of extracellular IL-2 by Tregs promotes Th17 differentiation (52). In addition to Tregs, the consumption of IL-2 by effector Th cells may limit the availability of IL-2 in the cellular microenvironment and prevent the paracrine effect of IL-2 on Th17 differentiation. In fact, IL-2 has been shown to promote clonal expansion and effector development of T cells in vivo and has been the growth-supporting cytokine in classical T cell clone–transferred EAE studies (63–65). Within Th17 cells, downregulation of IL-2 expression by TGF-β occurs by a SMAD-mediated inhibition of gene transcription (20–23). We found that during Th17 differentiation, miR-21 plays a significant role in the downregulation of IL-2 expression and that the antibody against IL-2 abrogated the observed defect in Th17 differentiation induced by *Mir21*$^{-/-}$ T cells. Therefore, our results suggest that miR-21 promotes the SMAD-mediated transcriptional downregulation of IL-2, acting as a positive regulator of Th17 differentiation. In the absence of miR-21, SMAD-7 levels are elevated, which in turn results in impaired TGF-β signaling, increased IL-2 expression, and the observed inhibition of Th17 differentiation (Figure 6). Thus, in addition to the T cell–extrinsic mechanism of IL-2 modulation, our results identify a T cell–intrinsic mechanism that limits the production of IL-2 to promote Th17 differentiation.

miR-21 was one the earliest identified "oncomirs," and therefore much of the research involving this miRNA has focused on its role in tumor promotion (66); however, our data build upon emerging reports establishing a crucial role for miR-21 in Th17-mediated autoimmunity. Specifically, our study corroborates the previous observation that miR-21 is overexpressed in the CNS-infiltrating T cells of animals with EAE (67) and is consistent with miR-21 involvement in other autoimmune disease models. For example, silencing miR-21 in vivo has led to a significant reduction of splenomegaly in lupus mice (68), targeted ablation of miR-21 has led to reduced lung eosinophilia after allergen challenge in mice (69), and most recently, *Mir21*$^{-/-}$ mice have been shown to be resistant to dextran sulfate sodium–induced (DSS-induced) colitis (70). Supporting these animal models, increased expression

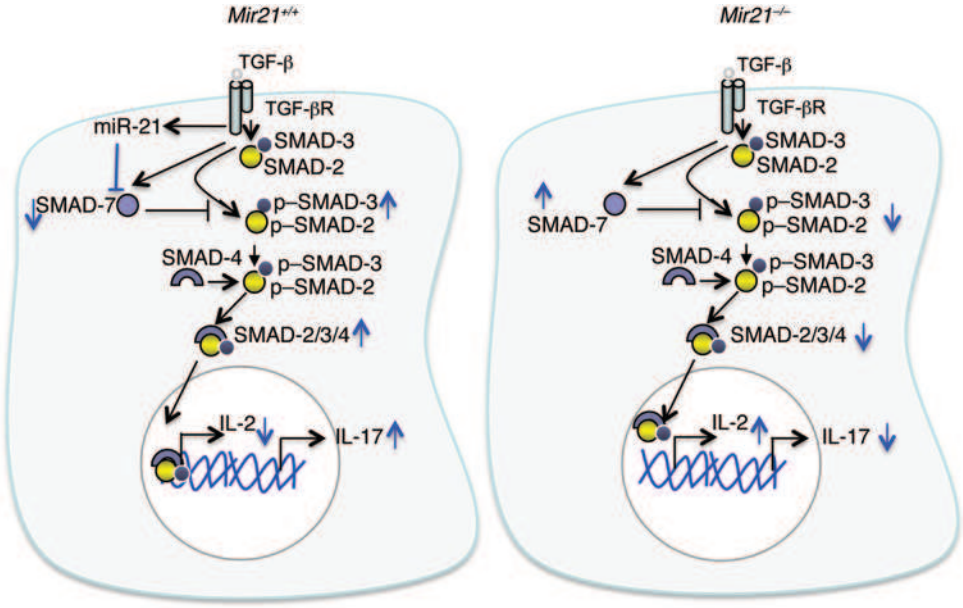

Figure 6. Model of molecular mechanisms involved in miR-21 regulation of Th17 differentiation. Our study demonstrates that miR-21 is increased in T cells stimulated under Th17-polarizing (TGF-β and IL-6) conditions. miR-21, in turn, promotes TGF-β signaling by targeting the inhibitory SMAD SMAD-7. The enhanced TGF-β signaling in WT T cells suppresses IL-2 expression and promotes their differentiation toward the Th17 phenotype. In the absence of miR-21, SMAD-7 levels are elevated, which in turn results in impaired TGF-β signaling, increased IL-2 expression, and the observed inhibition of Th17 differentiation. Black arrows indicate conventional TGF-β signaling in Th17 differentiation. Blue arrows indicate the modulation of TGF-β signaling in Th17 differentiation in the presence or absence of miR-21. Proposed pathways are shown in WT (*Mir21*$^{+/+}$) and miR-21–deficient (*Mir21*$^{-/-}$) T cells.

of miR-21 has been observed in peripheral blood mononuclear cells from patients with MS (27). Increased miR-21 levels have also been reported in T cells from patients with SLE and psoriasis (28–30), and these levels correlated with disease activity. Given the ameliorating effect of anti–miR-21 we observed in EAE, the implication of miR-21 in multiple autoimmune disease models, and the expression profile of miR-21 in patients with MS and other autoimmune diseases, silencing miR-21 may be an effective therapeutic approach in the treatment of MS and other Th17-mediated inflammatory diseases. In conclusion, we have identified a T cell–intrinsic miRNA pathway that enhances TGF-β signaling, limits the autocrine inhibitory effects of IL-2, and thereby promotes Th17 differentiation and autoimmunity.

Methods

Mice. C57BL/6, C57BL/6XSV129 (F1), *Smad7*$^{fl/fl}$, and *Cd4-Cre* mice were obtained from The Jackson Laboratory. *Mir21*$^{-/-}$ C57BL/6xSV129 (F1) mice were provided by Eric N. Olson (University of Texas Southwestern Medical Center, Dallas, Texas, USA).

Induction and evaluation of EAE. Mice were injected s.c. into both flanks with 100 μg $MOG_{35–55}$ peptide (MEVGWYRSPFSRVVHLYRNGK) dissolved in PBS emulsified in an equal volume of CFA (Difco) supplemented with 5 mg/ml *Mycobacterium tuberculosis* H37Ra. They were also injected twice i.p. with 200 ng PT (List Biological Laboratories) administered on the day of immunization and 48 hours later. Clinical assessment of EAE was performed daily after disease induction according to the following criteria: 0, no disease; 1, tail paralysis; 2, hind limb weakness or partial paralysis; 3, complete hind limb paralysis; 4, forelimb and hind limb paralysis; 5, moribund state. Mean clinical scores on separate days were calculated by adding the scores of individual mice and dividing by the total number of mice in each group, including mice that did not develop signs of EAE. For histopathological studies, spinal cords were dissected from female mice (n = 5/group), fixed in 10% formalin in PBS, and embedded in a single paraffin block. Sections (6–10 μm thick) were stained with H&E and Luxol fast blue. Stained sections were evaluated for immune cell infiltration and demyelination.

Proliferation assay. CellTrace Violet–labeled naive $CD4^+$ T cells were cultured in flat-bottom 96-well plates and stimulated with plate-bound anti-CD3 (2 μg/ml) and anti-CD28 (2 μg/ml). Cell proliferation was assessed by flow cytometry after 72 hours of culture using the Proliferation Platform analysis tool in FlowJo (version 9) software. We examined the following parameters, as defined by FlowJo software: Percent Divided, the fraction of original cell populations that have undergone at least 1 cell division; Division Index, average number of cell divisions that cells in the original cell population have undergone (includes undivided cells/peak); Proliferation Index, total number of cell divisions divided by the number of proliferating cells (excludes undivided cells/peak); Expansion Index, the fold-change expansion of the overall cultures (includes undivided cells/peak); and Replication Index, the fold-change expansion of only the proliferating cells (excludes undivided cells/peak). Alternatively, splenocyte suspensions were generated from $MOG_{35–55}$-immunized WT and *Mir21*$^{-/-}$ mice. Splenocytes from individual mice depleted of rbc were labeled with CellTrace Violet and plated (5×10^5 cells/well) in 200 μl Iscove's modified Dulbecco's medium (IMDM) with and without 25 μg/ml $MOG_{35–55}$ peptide. After 72 hours, proliferation of $MOG_{35–55}$-specific T cells was analyzed by flow cytometry.

IL-17 secretion assay. IL-17–secreting $CD4^+$ T cells were isolated using the Miltenyi Biotec Mouse IL-17 Secretion Assay – Cell Enrichment and Detection Kit. In brief, total $CD4^+$ T cells from $MOG_{35–55}$ peptide–immunized WT mice were stimulated with PMA plus ionomycin for 4 hours. Subsequently, an IL-17–specific catch reagent was attached to the cell surface of T cells. The cells were then incubated for 45 minutes at 37°C to allow cytokine secretion. The secreted IL-17 binds to the IL-17 catch reagent on the positive IL-17–secreting cells. These cells were subsequently labeled with a second IL-17–specific detection antibody, and $IL\text{-}17^+$ and $IL\text{-}17^-CD4^+$ T cells were sorted by flow cytometry.

Analysis of miR-21 expression. For analysis of miR-21 expression, real-time reverse transcription PCR (RT-PCR) was performed using TaqMan MicroRNA Assays (Applied Biosystems, Thermo Fisher Scientific). Relative expression was calculated using the Ct method and

normalized to uniformly expressed U6 snRNA or snoRNA135 (Applied Biosystems, Thermo Fisher Scientific). miR-21 values were expressed relative to the expression of U6 snRNA or snoRNA135. The levels of miR-21 in CNS-infiltrating T cells during peak EAE were normalized to T cells isolated from spleens of naive mice.

RNA isolation, cDNA synthesis, and real-time RT-PCR. Total RNA was isolated from cell pellets using the RNeasy Micro Kit (QIAGEN). RNA was stored at –80°C. First-strand cDNA synthesis was performed for each RNA sample from 0.5 to 1 μg of total RNA using TaqMan reverse transcription reagents. cDNA was amplified using sequence-specific primers. The probes used were identified by the following Applied Biosystems assay numbers: *Ifng*, Mm01168134_m1; *Il17a*, Mm99999062_m1; *Rorgt*, Mm01261019-m1; *Rora*, Mm00443103_m1; *Irf4*, Mm00516431_m1; *Batf*, Mm00479410_m1; *Hif1a*, Mm01283760_m1; *Il17f*, Mm00521423_m1; *Foxp3*, Mm00475151_m1; *Il4*, Mm00445259_m1; *Il23r*, Mm00519942_m1; *Il23*, Mm01160011_m1; *Il6*, Mm99999064_m1; *Il1b*, Mm01336189_m1; *Tnfa*, Mm00443258_m1; *Ccr6*, Mm01323931_m1; *Il6r*, Mm00439653_m1; *Tgfbr1*, Mm00436964_m1; *Tgfbr2*, Mm00436977_m1; *Il2*, Mm00434256_m1; *Btg2*, Mm00476162_m1; *Pdcd4*, Mm01266062_m1; *Pten*, Mm00477208_m1; *Spry1*, Mm01285700_m1; *Spry2*, Mm00442344_m1; and Real-Time PCR Mix (Applied Biosystems, Thermo Fisher Scientific) on the ABI7500 cycler. The *Gapdh* gene was used as an endogenous control to normalize for differences in the amount of total RNA in each sample. All values were expressed relative to *Gapdh* expression.

Anti–miR-21 treatment. An antisense oligonucleotide modified by LNA was synthesized to inhibit miR-21 (Exiqon). For in vivo anti–miR-21 treatment, anti–miR-21 and scrambled controls (30 μg/mouse) were administered i.v. to MOG-immunized mice on days 5, 7, 9, 11, and 13 after immunization.

Th differentiation. For in vitro Th17 cell differentiation, naive $CD4^+CD62L^{hi}CD44^{lo}$ T cells from WT and *Mir21*$^{-/-}$ mice were sorted by flow cytometry and activated with plate-bound anti-CD3 (2 μg/ml) and anti-CD28 (2 μg/ml) in the presence of TGF-β (2 ng/ml) and IL-6 (30 ng/ml). IL-2 activity in Th17 cell cultures was blocked with a combination of neutralizing anti–IL-2 (10 μg/ml) and blocking anti–CD25 (10 μg/ml) antibodies (BD Biosciences). For Th1 polarizations, naive $CD4^+$ T cells were activated with IL-12 (20 ng/ml) in the presence of anti–IL-4 (20 μg/ml) antibody (BD Biosciences). For Th2 polarizations, naive $CD4^+$ T cells were activated with IL-4 (20 ng/ml) in the presence of anti–IFN-γ (20 μg/ml) antibody (BD Biosciences). For iTreg differentiations, naive $CD4^+$ T cells were activated with TGF-β (5 ng/ml) in the presence of IL-2 (50 U/ml). Twenty-four hours after culture, transcription factor expression was analyzed by real-time RT-PCR. Five days after activation, cells were restimulated with PMA plus ionomycin for 4 hours for intracellular cytokine analysis by flow cytometry.

Generation and isolation of DCs. DCs were derived from BM progenitor cells. In brief, femoral and tibial cells were harvested in DC culture medium (RPMI 1640 medium, 10% FCS, 100 U/ml penicillin, 100 μg/ml streptomycin, 20 ng/ml GM-CSF, and 10 ng/ml IL-4) and seeded in 24-well plates at a density of 1×10^6 cells/ml/well. Culture medium was replaced with fresh medium after 3 days. On day 6, dislodged cells were used as BM-derived DCs. Splenic DCs were isolated from spleens using magnetic CD11c beads (Miltenyi Biotec).

Lentiviral shRNA transfection. $CD4^+$ T cells were cultured in the presence of lentiviral particles and polybrene (8 μg/ml) (Sigma-Aldrich). Cells were centrifuged at 900 *g* for 30 minutes at room temperature and incubated overnight. Cells were then centrifuged to remove the viral particles and cultured in fresh T cell differentiation medium. After 4 days, cells were analyzed for IL-17 expression by flow cytometry.

$CD4^+$ T cell transfer. $CD4^+$ T cells were prepared from the spleens and inguinal LNs of WT and *Mir21*$^{-/-}$ mice using the $CD4^+$ T Cell Isolation Kit (Miltenyi Biotec) (purity was >95%). $CD4^+$ T cells (2×10^7 cells/mouse) were injected i.v. into WT or *Mir21*$^{-/-}$ mice. Five days later, the recipient mice were subjected to EAE induction. For Th1- and Th17-mediated EAE, WT and *Mir21*$^{-/-}$ mice were immunized with $MOG_{35–55}$ peptide emulsified in CFA. Ten days after immunization, mice were sacrificed, and $CD4^+$ T cells from spleens and inguinal LNs were cultured for 5 days in the presence of 50 μg/ml MOG peptide and 20 ng/ml IL-23 to generate Th17 cells, or with MOG peptide and 20 ng/ml IL-12 to generate Th1 cells. Naive 2D2 $CD4^+$ T cell–polarized Th17 cells in the presence or absence of miR-21 inhibitors (2×10^7 cells per mouse) were transferred into naive mice. Transplanted mice were injected with PT on the day of T cell transfer and again 48 hours later. EAE progression was monitored as described above.

Preparation and evaluation of CNS cells. Animals were perfused with cold PBS. Brains and spinal cords were dissected and incubated in 2.5 mg/ml collagenase D for 30 minutes at 37°C. Single-cell suspensions were prepared by passing them through a 70-μm strainer. Cells were washed in RPMI 1640 medium, and mononuclear cells were isolated using a discontinuous Percoll gradient (Pharmacia). Cells were washed twice, and $CD4^+$ T cells were isolated from this suspension by magnetic separation using microbeads (Miltenyi Biotec).

Luciferase assay. Semiconfluent (70%–80%) HEK-293 cells were cotransfected with pRL-GAPDH (gift of Matthias Brock, Center of Experimental Rheumatology, University Hospital Zurich, Switzerland) and SMAD-7 WT or mutant luciferase constructs using DharmaFECT Duo Transfection Reagent (GE Healthcare) according to the manufacturer's instructions, washed 6 hours after transfection, and incubated for 24 hours. Cells were then lysed by passive lysis buffer, and luminescence was measured using the Dual-Glo Luciferase Assay System (Promega) on a Veritas Luminometer (Turner BioSystems). SMAD-7 luciferase readings (firefly luciferase) were normalized to GAPDH luciferase (*Renilla* luciferase) readings, and fold changes were calculated as compared with those in control cells.

MOG tetramer staining. Splenocytes derived from WT and *Mir21*$^{-/-}$ mice immunized with $MOG_{35–55}$ peptide were harvested at disease onset and stained with $MOG_{38–49}$-PE tetramer (1:100) or control tetramer–PE (NIH Tetramer Facility) for 2 hours at room temperature in IMDM and analyzed by flow cytometry.

Immunoblotting. Naive $CD4^+$ T cells were stimulated for 24 hours with plate-bound anti-CD3 and anti-CD28. After a 16-hour resting period, cells were stimulated with TGF-β (2 ng/ml) at the indicated time points (Figure 4, A and B). Cells were homogenized in RIPA buffer (50 mM Tris-HCl, pH 7.4, 150 mM NaCl, 1% NP40), 1X protease inhibitor cocktail (Roche Applied Science), and 1X phosphatase inhibitor cocktail (Sigma-Aldrich), and equal amounts of protein (25 μg) were resolved by polyacrylamide gel electrophoresis. Proteins were transferred onto a nitrocellulose membrane, and immunoblotting was performed with mouse monoclonal anti–SMAD-7 (R&D Systems), GAPDH and α-tubulin (Sigma-Aldrich), rabbit polyclonal p–SMAD-2, p–SMAD-2, SMAD-3, p-p38MAPK, p-ERK, p-JNK, p38MAPK, ERK, and JNK antibodies (Cell Signaling Technology).

SMAD-7 HRP–conjugated secondary antibodies against mouse or rabbit were purchased from Jackson ImmunoResearch. Images were captured using the Bio-Rad ChemiDoc MP imaging system.

Statistics. Statistical analysis was performed using the unpaired 2-tailed Student's *t* test. A *P* value of less than 0.05 was considered statistically significant. Data are presented as the mean ± SEM. For EAE, groups were compared using linear regression analysis.

Study approval. Animals were maintained in specific pathogen–free conditions in the animal facility of Harvard Institutes of Medicine. All mice were 6–10 weeks of age at the beginning of the experiments. All Experiments were reviewed and approved by the IACUC of Harvard Medical School.

Acknowledgments

We thank E.N. Olson (University of Texas Southwestern Medical Center, Dallas, Texas, USA) for the *Mir21*$^{-/-}$ mice; M. Brock (Center of Experimental Rheumatology, University Hospital Zurich) for pRL-GAPDH, and G. Liu (University of Alabama at Birmingham, Birmingham, Alabama, USA) for the SMAD-7 WT and mutant luciferase constructs. This work was supported by grants from the NIH (AI435801 and NS38037, to H.L. Weiner); the Nancy Davis Foundation for MS (to G. Murugaiyan); the National Multiple Sclerosis Society (RG 4904A2/1, to G. Murugaiyan); and the Swiss National Science Foundation (PP00P3_150663, to N. Joller). The Vaidya laboratory is supported by an NIH Outstanding New Environmental Scientist Award (ES017543).

Address correspondence to: Gopal Murugaiyan or Howard L. Weiner, Ann Romney Center for Neurologic Diseases, Brigham and Women's Hospital and Harvard Medical School, HIM 720, 77 Avenue Louis Pasteur, Boston, Massachusetts 02115, USA. Phone: 617.849.0912; E-mail: mgopal@rics.bwh.harvard.edu (G. Murugaiyan). Phone: 617.525.5300; E-mail: hweiner@rics.bwh.harvard.edu (H.L. Weiner).

1. Korn T, Bettelli E, Oukka M, Kuchroo VK. IL-17 and Th17 Cells. *Annu Rev Immunol*. 2009;27:485–517.
2. Langrish CL, et al. IL-23 drives a pathogenic T cell population that induces autoimmune inflammation. *J Exp Med*. 2005;201(2):233–240.
3. Steinman L. A brief history of T(H)17, the first major revision in the T(H)1/T(H)2 hypothesis of T cell-mediated tissue damage. *Nat Med*. 2007;13(2):139–145.
4. Becher B, Segal BM. T(H)17 cytokines in autoimmune neuro-inflammation. *Curr Opin Immunol*. 2011;23(6):707–712.
5. Tzartos JS, et al. Interleukin-17 production in central nervous system-infiltrating T cells and glial cells is associated with active disease in multiple sclerosis. *Am J Pathol*. 2008;172(1):146–155.
6. Mangan PR, et al. Transforming growth factor-beta induces development of the T(H)17 lineage. *Nature*. 2006;441(7090):231–234.
7. Bettelli E, et al. Reciprocal developmental pathways for the generation of pathogenic effector TH17 and regulatory T cells. *Nature*. 2006;441(7090):235–238.
8. Veldhoen M, Hocking RJ, Atkins CJ, Locksley RM, Stockinger B. TGFβ in the context of an inflammatory cytokine milieu supports de novo differentiation of IL-17-producing T cells. *Immunity*. 2006;24(2):179–189.
9. Korn T, et al. IL-21 initiates an alternative pathway to induce proinflammatory T(H)17 cells. *Nature*. 2007;448(7152):484–487.
10. Nurieva R, et al. Essential autocrine regulation by IL-21 in the generation of inflammatory T cells. *Nature*. 2007;448(7152):480–483.
11. Ghoreschi K, et al. Generation of pathogenic T(H)17 cells in the absence of TGF-beta signalling. *Nature*. 2010;467(7318):967–971.
12. Ivanov II, et al. The orphan nuclear receptor RORgammat directs the differentiation program of proinflammatory IL-17^{+} T helper cells. *Cell*. 2006;126(6):1121–1133.
13. Yang XO, et al. T helper 17 lineage differentiation is programmed by orphan nuclear receptors RORα and RORγ. *Immunity*. 2008;28(1):29–39.
14. Huber M, et al. IRF4 is essential for IL-21-mediated induction, amplification, and stabilization of the Th17 phenotype. *Proc Natl Acad Sci U S A*. 2008;105(52):20846–20851.
15. Schraml BU, et al. The AP-1 transcription factor Batf controls T(H)17 differentiation. *Nature*. 2009;460(7253):405–409.
16. Dang EV, et al. Control of T(H)17/T(reg) balance by hypoxia-inducible factor 1. *Cell*. 2011;146(5):772–784.
17. Veldhoen M, Hocking RJ, Flavell RA, Stockinger B. Signals mediated by transforming growth factor-β initiate autoimmune encephalomyelitis, but chronic inflammation is needed to sustain disease. *Nat Immunol*. 2006;7(11):1151–1156.
18. Shi Y, Massague J. Mechanisms of TGF-β signaling from cell membrane to the nucleus. *Cell*. 2003;113(6):685–700.
19. Malhotra N, Robertson E, Kang J. SMAD2 is essential for TGFβ-mediated Th17 cell generation. *J Biol Chem*. 2010;285(38):29044–29048.
20. Meisel M, et al. The kinase PKCα selectively upregulates interleukin-17A during Th17 cell immune responses. *Immunity*. 2013;38(1):41–52.
21. Cejas PJ, et al. TRAF6 inhibits Th17 differentiation and TGF-β-mediated suppression of IL-2. *Blood*. 2010;115(23):4750–4757.
22. McKarns SC, Schwartz RH, Kaminski NE. Smad3 is essential for TGF-β1 to suppress IL-2 production and TCR-induced proliferation, but not IL-2-induced proliferation. *J Immunol*. 2004;172(7):4275–4284.
23. Liao W, Lin JX, Wang L, Li P, Leonard WJ. Modulation of cytokine receptors by IL-2 broadly regulates differentiation into helper T cell lineages. *Nat Immunol*. 2011;12(6):551–559.
24. Ambros V. The functions of animal microRNAs. *Nature*. 2004;431(7006):350–355.
25. Zare-Shahabadi A, Renaudineau Y, Rezaei N. MicroRNAs and multiple sclerosis:from physiopathology toward therapy. *Expert Opin Ther Targets*. 2013;17(12):1497–1507.
26. O'Connell RM, Rao DS, Chaudhuri AA, Baltimore D. Physiological and pathological roles for microRNAs in the immune system. Nature reviews. *Immunology*. 2010;10(2):111–122.
27. Fenoglio C, et al. Expression and genetic analysis of miRNAs involved in CD4^{+} cell activation in patients with multiple sclerosis. *Neurosci Lett*. 2011;504(1):9–12.
28. Stagakis E, et al. Identification of novel microRNA signatures linked to human lupus disease activity and pathogenesis: miR-21 regulates aberrant T cell responses through regulation of PDCD4 expression. *Ann Rheum Dis*. 2011;70(8):1496–1506.
29. Wang H, Peng W, Ouyang X, Li W, Dai Y. Circulating microRNAs as candidate biomarkers in patients with systemic lupus erythematosus. *Transl Res*. 2012;160(3):198–206.
30. Meisgen F, et al. MiR-21 is up-regulated in psoriasis and suppresses T cell apoptosis. *Exp Dermatol*. 2012;21(4):312–314.
31. Reboldi A, et al. C-C chemokine receptor 6-regulated entry of TH-17 cells into the CNS through the choroid plexus is required for the initiation of EAE. *Nat Immunol*. 2009;10(5):514–523.
32. Sheedy FJ, et al. Negative regulation of TLR4 via targeting of the proinflammatory tumor suppressor PDCD4 by the microRNA miR-21. *Nat Immunol*. 2010;11(2):141–147.
33. Frankel LB, Christoffersen NR, Jacobsen A, Lindow M, Krogh A, Lund AH. Programmed cell death 4 (PDCD4) is an important functional target of the microRNA miR-21 in breast cancer cells. *J Biol Chem*. 2008;283(2):1026–1033.
34. Lu Z, et al. MicroRNA-21 promotes cell transformation by targeting the programmed cell death 4 gene. *Oncogene*. 2008;27(31):4373–4379.
35. Liu M, et al. Regulation of the cell cycle gene, BTG2, by miR-21 in human laryngeal carcinoma. *Cell Res*. 2009;19(7):828–837.
36. Thum T, et al. MicroRNA-21 contributes to myocardial disease by stimulating MAP kinase signalling in fibroblasts. *Nature*. 2008;456(7224):980–984.
37. Polytarchou C, et al. Akt2 regulates all Akt isoforms and promotes resistance to hypoxia through induction of miR-21 upon oxygen deprivation. *Cancer Res*. 2011;71(13):4720–4731.
38. Meng F, Henson R, Wehbe-Janek H, Ghoshal K, Jacob ST, Patel T. icroRNA-21 regulates expression of the PTEN tumor suppressor gene in

human hepatocellular cancer. *Gastroenterology*. 2007;133(2):647–658.
39. Iliopoulos D, Jaeger SA, Hirsch HA, Bulyk ML, Struhl K. STAT3 activation of miR-21 and miR-181b-1 via PTEN and CYLD are part of the epigenetic switch linking inflammation to cancer. *Mol Cell*. 2010;39(4):493–506.
40. Awasthi A, et al. Cutting edge:IL-23 receptor gfp reporter mice reveal distinct populations of IL-17-producing cells. *J Immunol*. 2009;182(10):5904–5908.
41. Sutton CE, Mielke LA, Mills KH. IL-17-producing γδ T cells and innate lymphoid cells. *Eur J Immunol*. 2012;42(9):2221–2231.
42. El-Behi M, et al. The encephalitogenicity of T(H)17 cells is dependent on IL-1- and IL-23-induced production of the cytokine GM-CSF. *Nat Immunol*. 2011;12(6):568–575.
43. McGeachy MJ. GM-CSF:the secret weapon in the T(H)17 arsenal. *Nat Immunol*. 2011;12(6):521–522.
44. Codarri L, et al. RORγt drives production of the cytokine GM-CSF in helper T cells, which is essential for the effector phase of autoimmune neuroinflammation. *Nat Immunol*. 2011;12(6):560–567.
45. Brüstle A, et al. The NF-κB regulator MALT1 determines the encephalitogenic potential of Th17 cells. *J Clin Invest*. 2012;122(12):4698–4709.
46. Yang XO, et al. STAT3 regulates cytokine-mediated generation of inflammatory helper T cells. *J Biol Chem*. 2007;282(13):9358–9363.
47. Liu G, et al. miR-21 mediates fibrogenic activation of pulmonary fibroblasts and lung fibrosis. *J Exp Med*. 2010;207(8):1589–1597.
48. Zhong X, et al. miR-21 is a key therapeutic target for renal injury in a mouse model of type 2 diabetes. *Diabetologia*. 2013;56(3):663–674.
49. Brabletz T, Pfeuffer I, Schorr E, Siebelt F, Wirth T, Serfling E. Transforming growth factor β and cyclosporin A inhibit the inducible activity of the interleukin-2 gene in T cells through a non-canonical octamer-binding site. *Mol Cell Biol*. 1993;13(2):1155–1162.
50. Tzachanis D, et al. Tob is a negative regulator of activation that is expressed in anergic and quiescent T cells. *Nat Immunol*. 2001;2(12):1174–1182.
51. Laurence A, et al. Interleukin-2 signaling via STAT5 constrains T helper 17 cell generation. *Immunity*. 2007;26(3):371–381.
52. Chen Y, et al. Foxp3(+) regulatory T cells promote T helper 17 cell development in vivo through regulation of interleukin-2. *Immunity*. 2011;34(3):409–421.
53. Murugaiyan G, Beynon V, Mittal A, Joller N, Weiner HL. Silencing microRNA-155 ameliorates experimental autoimmune encephalomyelitis. *J Immunol*. 2011;187(5):2213–2221.
54. Elmen J, et al. LNA-mediated microRNA silencing in non-human primates. *Nature*. 2008;452(7189):896–899.
55. Bernardo BC, et al. Therapeutic inhibition of the miR-34 family attenuates pathological cardiac remodeling and improves heart function. *Proc Natl Acad Sci U S A*. 2012;109(43):17615–17620.
56. Wan YY, Flavell RA. 'Yin-Yang' functions of transforming growth factor-beta and T regulatory cells in immune regulation. *Immunol Rev*. 2007;220:199–213.
57. Takimoto T, et al. Smad2 and Smad3 are redundantly essential for the TGF-β-mediated regulation of regulatory T plasticity and Th1 development. *J Immunol*. 2010;185(2):842–855.
58. Lu L, et al. Role of SMAD and non-SMAD signals in the development of Th17 and regulatory T cells. *J Immunol*. 2010;184(8):4295–4306.
59. Schlenner SM, Weigmann B, Ruan Q, Chen Y, von Boehmer H. Smad3 binding to the foxp3 enhancer is dispensable for the development of regulatory T cells with the exception of the gut. *J Exp Med*. 2012;209(9):1529–1535.
60. Gu AD, Wang Y, Lin L, Zhang SS, Wan YY. Requirements of transcription factor Smad-dependent and -independent TGF-β signaling to control discrete T-cell functions. *Proc Natl Acad Sci U S A*. 2012;109(3):905–910.
61. Huber S, et al. P38 MAP kinase signaling is required for the conversion of $CD4^+CD25^-$ T cells into iTreg. *PLoS One*. 2008;3(10):e3302.
62. Quintana FJ, et al. Aiolos promotes TH17 differentiation by directly silencing Il2 expression. *Nat Immunol*. 2012;13(8):770–777.
63. Liao W, Lin JX, Leonard WJ. Interleukin-2 at the crossroads of effector responses, tolerance, and immunotherapy. *Immunity*. 2013;38(1):13–25.
64. Cravens PD, et al. Lymph node-derived donor encephalitogenic $CD4^+$ T cells in C57BL/6 mice adoptive transfer experimental autoimmune encephalomyelitis highly express GM-CSF and T-bet. *J Neuroinflammation*. 2011;8:73.
65. Jager A, Dardalhon V, Sobel RA, Bettelli E, Kuchroo VK. Th1, Th17, and Th9 effector cells induce experimental autoimmune encephalomyelitis with different pathological phenotypes. *J Immunol*. 2009;183(11):7169–7177.
66. Si ML, Zhu S, Wu H, Lu Z, Wu F, Mo YY. miR-21-mediated tumor growth. *Oncogene*. 2007;26(19):2799–2803.
67. Mycko MP, Cichalewska M, Machlanska A, Cwiklinska H, Mariasiewicz M, Selmaj KW. MicroRNA-301a regulation of a T-helper 17 immune response controls autoimmune demyelination. *Proc Natl Acad Sci U S A*. 2012;109(20):E1248– E1257.
68. Garchow BG, et al. Silencing of microRNA-21 in vivo ameliorates autoimmune splenomegaly in lupus mice. *EMBO Mol Med*. 2011;3(10):605–615.
69. Lu TX, et al. MicroRNA-21 limits in vivo immune response-mediated activation of the IL-12/IFN-γ pathway, Th1 polarization, and the severity of delayed-type hypersensitivity. *J Immunol*. 2011;187(6):3362–3373.
70. Shi C, et al. MicroRNA-21 knockout improve the survival rate in DSS induced fatal colitis through protecting against inflammation and tissue injury. *PLoS One*. 2013;8(6):e66814.

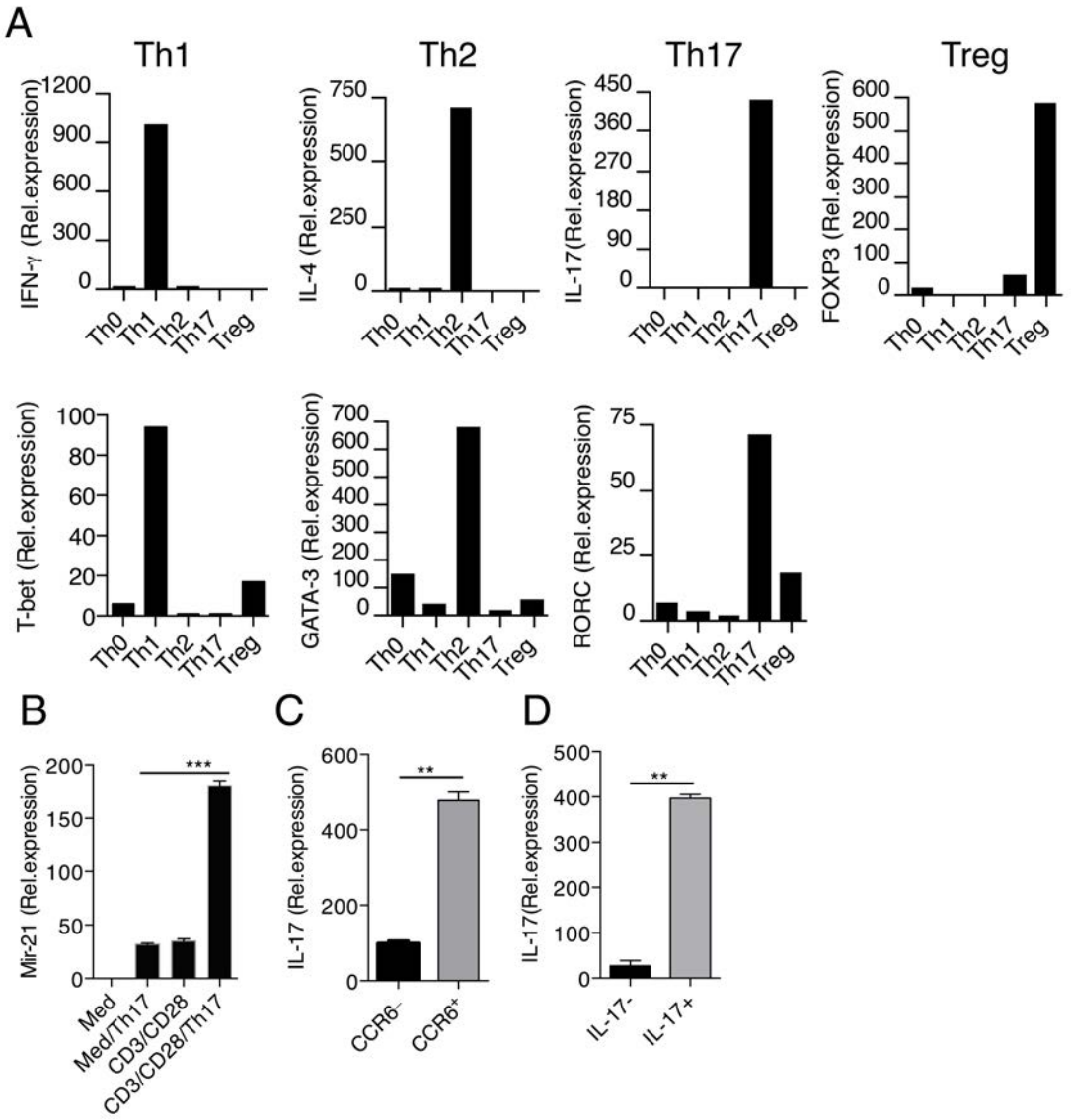

Supplemental Figure 1. Signature gene expression in in vitro differentiated Th0, Th1, Th2, Th17 and Treg cells. **(A)** Naïve $CD4^+$ T cells were cultured under Th0, Th1, Th2, Th17, and Treg conditions. mRNA levels of specific transcription factors and cytokines were analyzed by quantitative RT-PCR. (**B**) Quantitative RT-PCR analysis of Mir-21 expression in naïve $CD4^+$ T cells activated with plate bound anti-CD3 (2 μg/ml) and anti-CD28 (2 μg/ml) in the presence or absence of Th17-polarizing conditions. (**C**) $CCR6^+$ and $CCR6^-$ populations were sorted from the in vitro differentiated Th17 culture and expression of IL17 was assessed by quantitative RT-PCR. (**D**) $IL\text{-}17^+$ and $IL\text{-}17^-$ populations were sorted using a mouse IL-17 secretion assay and expression of IL17 was assessed by quantitative RT-PCR. Data are from two independent experiments. Error bars, mean ± SEM. *p<0.05, **p<0.01, ***p<0.001, unpaired Student's *t* test.

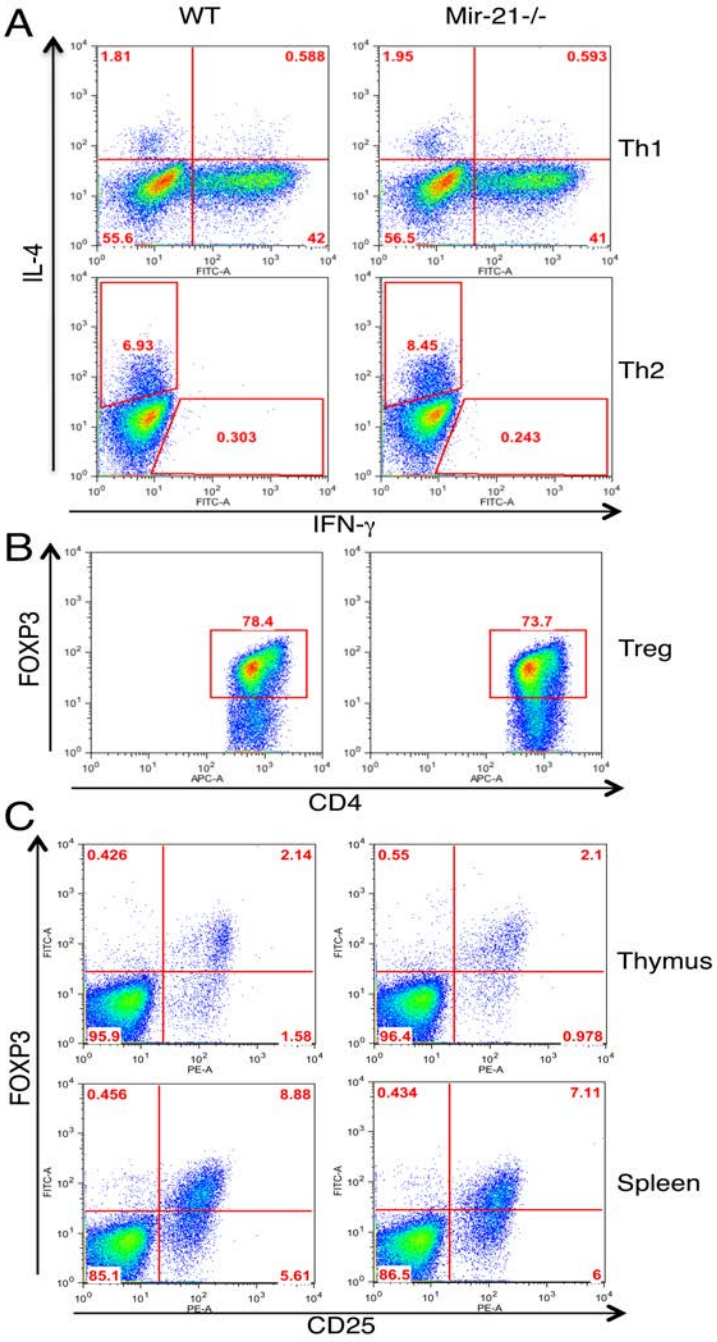

Supplemental Figure 2. Mir-21 deficiency does not affect Th1, Th2, and Treg cells. (A) WT and Mir-21$^{-/-}$ derived naïve CD4^{+} T cells cultured under Th1 and Th2 conditions were restimulated with PMA/ionomycin on day 5 and stained for IL-4 and IFN-γ. Numbers represent the frequency of CD4^{+} T cells. (**B**) WT and Mir-21$^{-/-}$-derived naïve CD4^{+} T cells cultured under iTreg conditions were stained for Foxp3. Numbers represent the frequency of CD4^{+} T cells. (**C**) Representative FACS plots display CD25^{+} Foxp3^{+} natural Treg (nTreg) cells in the thymus and spleen. Numbers represent the frequency of CD4^{+} T cells. Data are representative of three independent experiments.

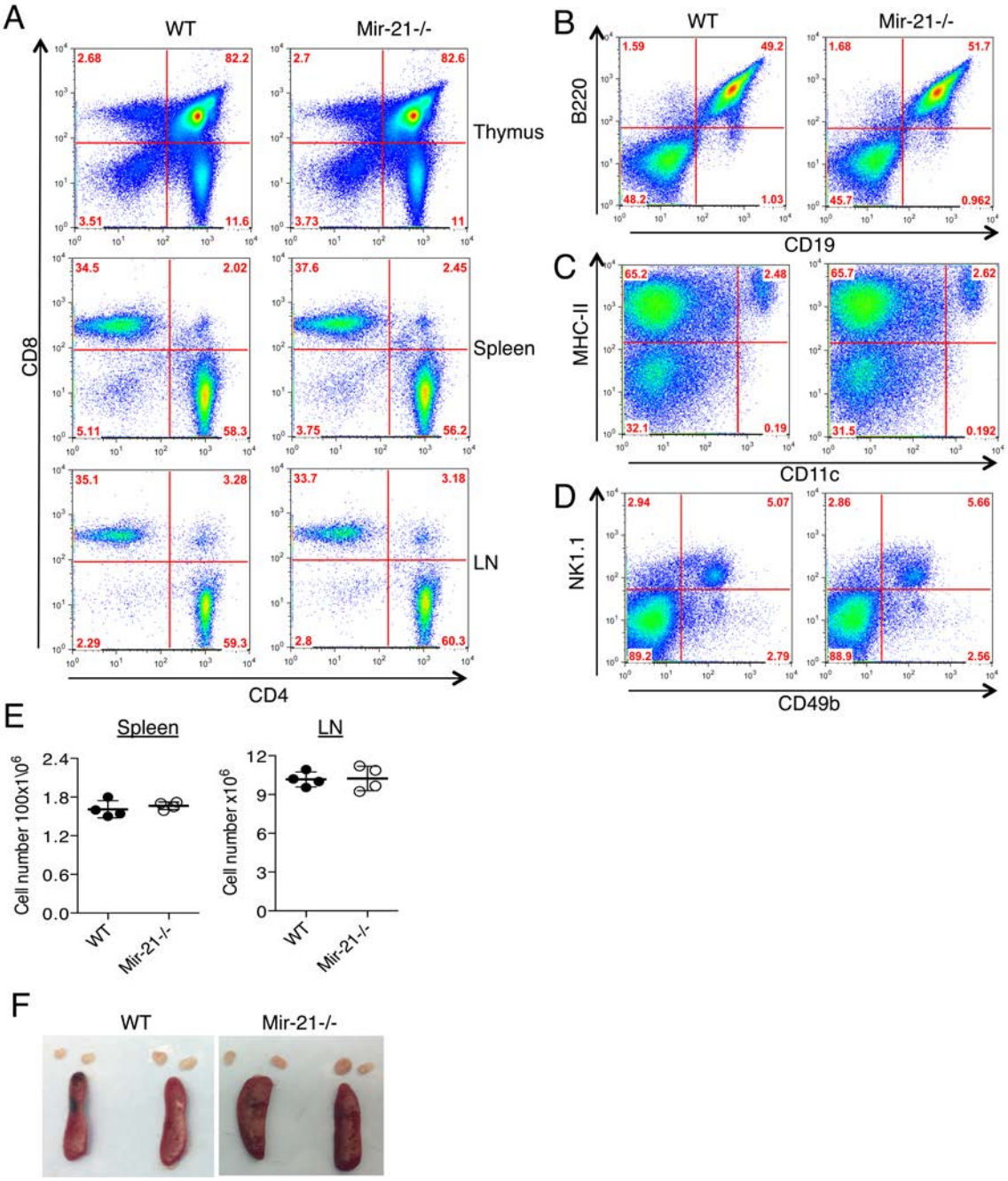

Supplemental Figure 3. **Mir-21 deficiency does not cause any apparent global immune abnormalities in terms of myeloid and lymphoid cell subsets (A)** Frequency of CD4 and CD8 double positive and CD4 and CD8 single positive T cells from thymus, spleen, and LN (**B-D**) Frequency of $B220^{+}$ $CD19^{+}$ B cells, $CD11c^{+}MHC\text{-}II^{+}$ DCs, and $NK1.1^{+}CD49b^{+}$ NK cells in spleen (**E**) Total cellularity of spleen and LN from 6-8 week-old WT and Mir-$21^{-/-}$ mice. (**F**) Gross morphology of spleens and LN. Data are representative of two independent experiments.

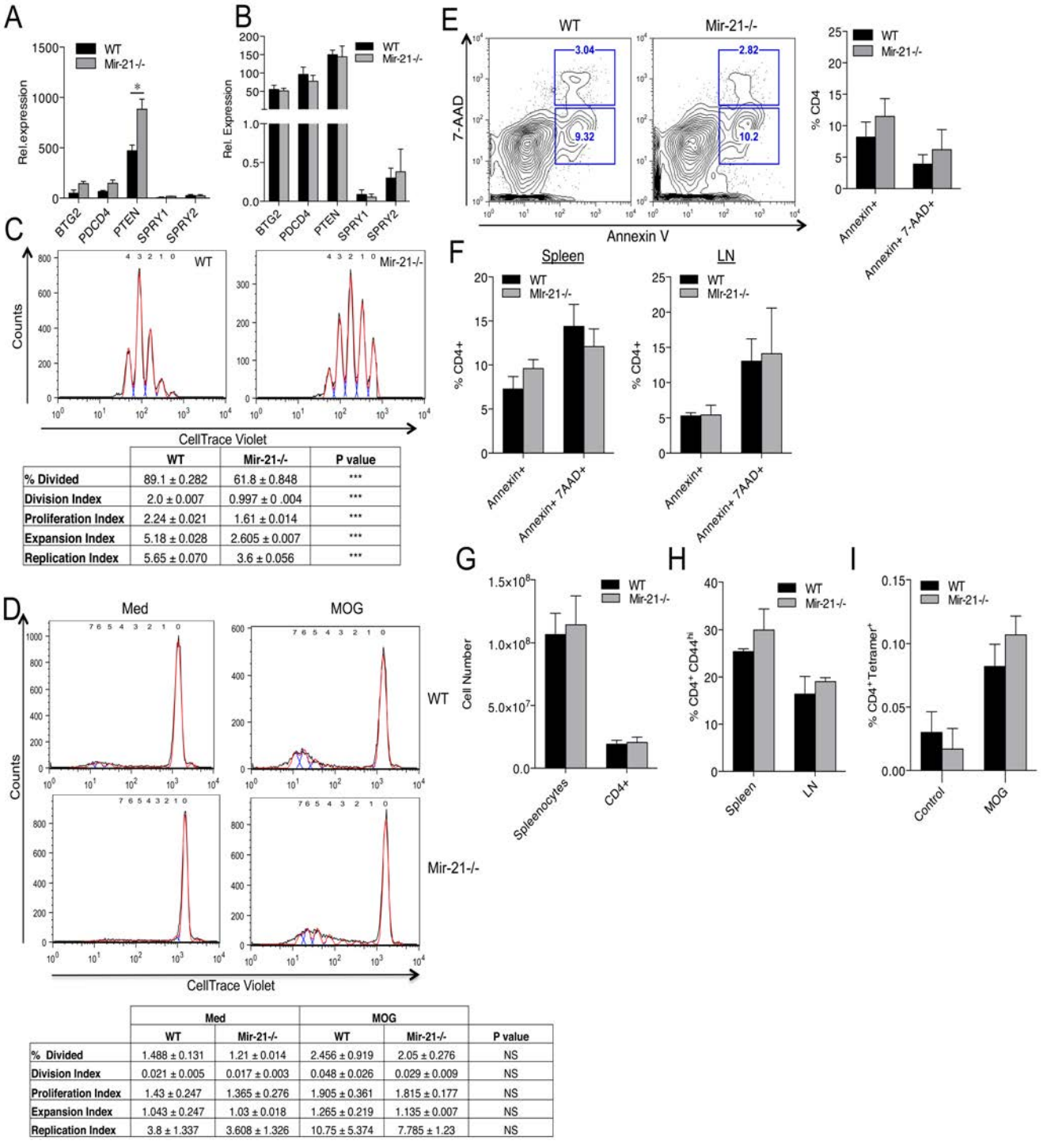

	WT	Mir-21-/-	P value
% Divided	89.1 ± 0.282	61.8 ± 0.848	***
Division Index	2.0 ± 0.007	0.997 ± 0 .004	***
Proliferation Index	2.24 ± 0.021	1.61 ± 0.014	***
Expansion Index	5.18 ± 0.028	2.605 ± 0.007	***
Replication Index	5.65 ± 0.070	3.6 ± 0.056	***

	Med		MOG		
	WT	Mir-21-/-	WT	Mir-21-/-	P value
% Divided	1.488 ± 0.131	1.21 ± 0.014	2.456 ± 0.919	2.05 ± 0.276	NS
Division Index	0.021 ± 0.005	0.017 ± 0.003	0.048 ± 0.026	0.029 ± 0.009	NS
Proliferation Index	1.43 ± 0.247	1.365 ± 0.276	1.905 ± 0.361	1.815 ± 0.177	NS
Expansion Index	1.043 ± 0.247	1.03 ± 0.018	1.265 ± 0.219	1.135 ± 0.007	NS
Replication Index	3.8 ± 1.337	3.608 ± 1.326	10.75 ± 5.374	7.785 ± 1.23	NS

Supplemental Figure 4. **Mir-21 deficiency does not affect antigen specific expansion of T cells.** (A). Real-time PCR analysis of Mir-21 targets btg2, pten, pdcd-4, spry1, and spry2 in WT and Mir-21$^{-/-}$ T cells stimulated with plate-bound anti-CD3 and anti-CD28 antibodies (2μg/ml). (B) Real-time PCR analysis of Mir-21 targets btg2, pten, pdcd-4, spry1, and spry2 in CD4^{+} T cells isolated from MOG_{35-55} immunized WT and Mir-21$^{-/-}$ mice. (C) Naïve CD4^{+} T cells from WT and Mir-21$^{-/-}$ mice were labeled with CellTrace Violet and stimulated in the presence of plate bound anti-CD3 and anti-CD28 antibodies (2μg/ml) for 72 hours. Proliferating T cells were analyzed by flow cytometry. (D) Splenocytes from MOG-immunized WT and Mir-21$^{-/-}$ mice were labeled with CellTrace Violet and stimulated in the presence or absence of MOG_{35-55} peptide (25 μg/ml) for 72 hours. Proliferating CD4^{+} T cells from both groups were analyzed by flow cytometry. (E) The percentage of annexin V^{+} and 7-amino-actinomycin D^{+} (7AAD^{+}) CD4^{+} T cells are shown (F) Frequencies of annexin V^{+} and annexin V^{+} 7-amino-actinomycin D^{+} (7AAD^{+}) CD4^{+} T cells from spleen and LN of MOG_{35-55} - immunized WT and Mir-21$^{-/-}$ mice (n=3). (G) Total cellularity of splenocytes and CD4^{+} cells in MOG_{35-55}-immunized WT and Mir-21$^{-/-}$ mice (n=3). (H) Frequency of activated CD4^{+} T cells from spleen and LN of MOG_{35-55}-immunized WT and Mir-21$^{-/-}$ mice (n=3). (I) Frequency of MOG tetramer^{+} T cells from spleen of MOG_{35-55}-immunized WT and Mir-21$^{-/-}$ mice (n=3). Data are representative of three independent experiments. Error bars, mean ± SEM. *p<0.05, **p<0.01, ***p<0.001, unpaired Student's *t* test.

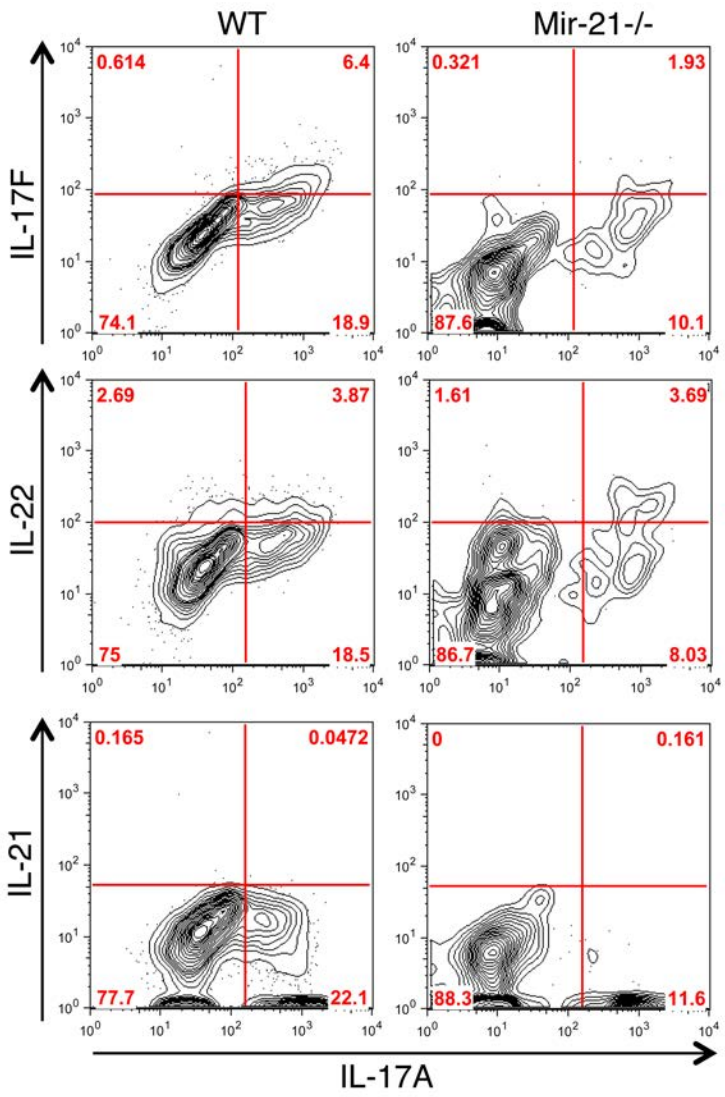

Supplemental Figure 5. Defective Th17 cytokine expression in CNS infiltrating T cells from Mir-21$^{-/-}$ mice. FACS analysis of IL-17A, IL-17F, IL-21, and IL-22 expression in CNS-infiltrating T cells from WT and Mir-21$^{-/-}$ mice with peak EAE (n=3). Numbers represent the frequency of CD4^{+} T cells. Data are representative of three independent experiments.

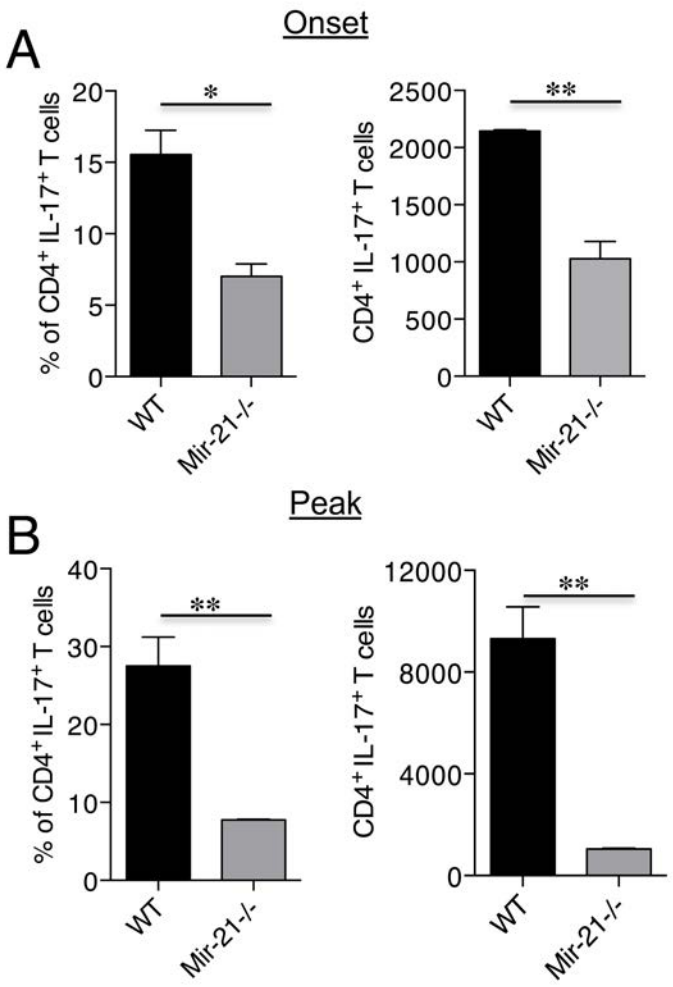

Supplemental Figure 6. Diminished frequencies and absolute numbers of Th17 cells in Mir-21$^{-/-}$ mice with EAE. IL-17 production by CNS-infiltrating CD4^{+} T cells from WT and Mir-21$^{-/-}$ mice with onset and peak EAE (n=3). CNS infiltrating CD4^{+} T cells were stimulated for 4 hr with PMA plus ionomycin in the presence of Golgi stop and analyzed for IL-17 expression. Data are representative of two independent experiments. Error bars, mean ± SEM. *p<0.05, **p<0.01, ***p<0.001, unpaired Student's *t* test.

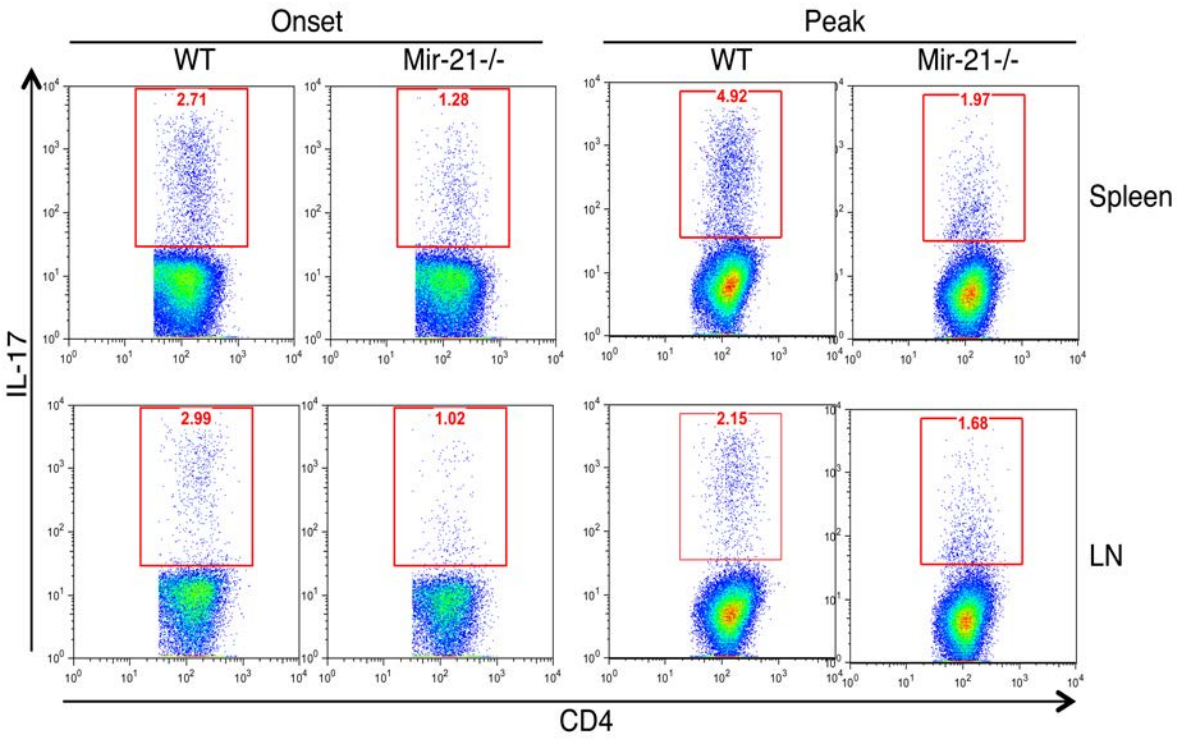

Supplemental Figure 7. Diminished frequencies of Th17 cells in the periphery of Mir-21$^{-/-}$ mice with EAE. FACS analysis of frequencies of IL-17 producing CD4^{+} T cells from spleen and LN of WT and Mir-21$^{-/-}$ mice with onset and peak EAE. Spleen and LN cells were stimulated for 4 hr with PMA plus ionomycin in the presence of Golgi stop and analyzed for IL-17 expression. Data are representative of two independent experiments.

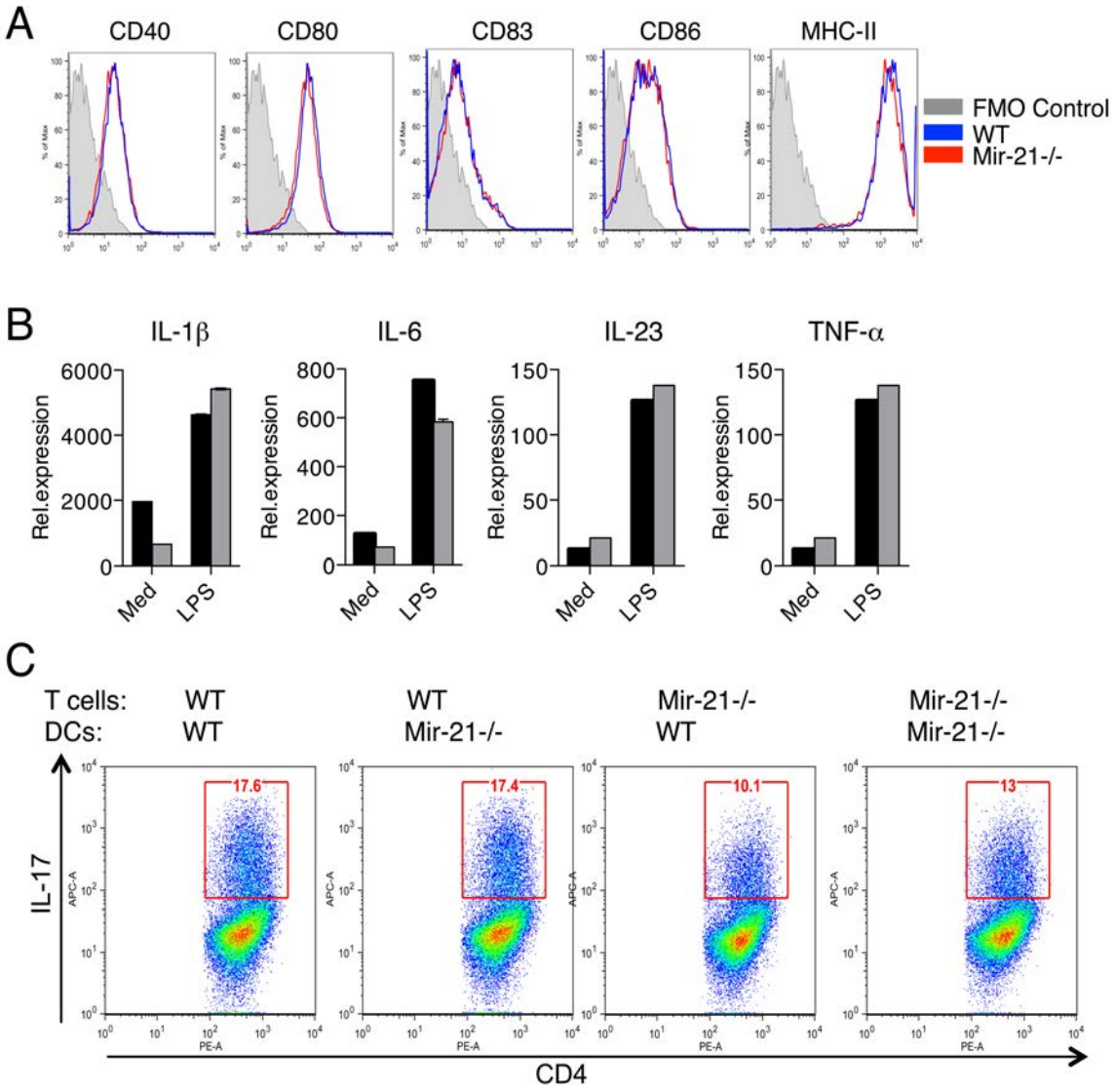

Supplemental Figure 8. Mir-21$^{-/-}$ dendritic cells (DCs) display an unimpaired phenotype. (A) The DC markers CD40, CD80, CD86, and MHC-II are appropriately expressed on the surface of Mir-21$^{-/-}$ DCs compared to WT DCs. DCs were stained for CD11C, MHCII, CD40, CD80, and CD86 and analyzed by flow cytometry. Histograms represent frequency of CD11c^{+} cells. **(B)** LPS-stimulated Mir-21$^{-/-}$ DCs express normal levels of the Th17-polarizing cytokines IL-1β, IL-6, IL-23, and TNF-α. The data are representative of two independent experiments. (**C**) CD4^{+} T cells isolated from WT and Mir-21$^{-/-}$ mice were co-cultured with CD11c^{+} DCs derived from WT and Mir-21$^{-/-}$ mice for 5 days and IL-17 expression in CD4^{+} T cells was analyzed by flow cytometry. Numbers represent frequency of CD4^{+} T cells. Data are from two independent experiments.

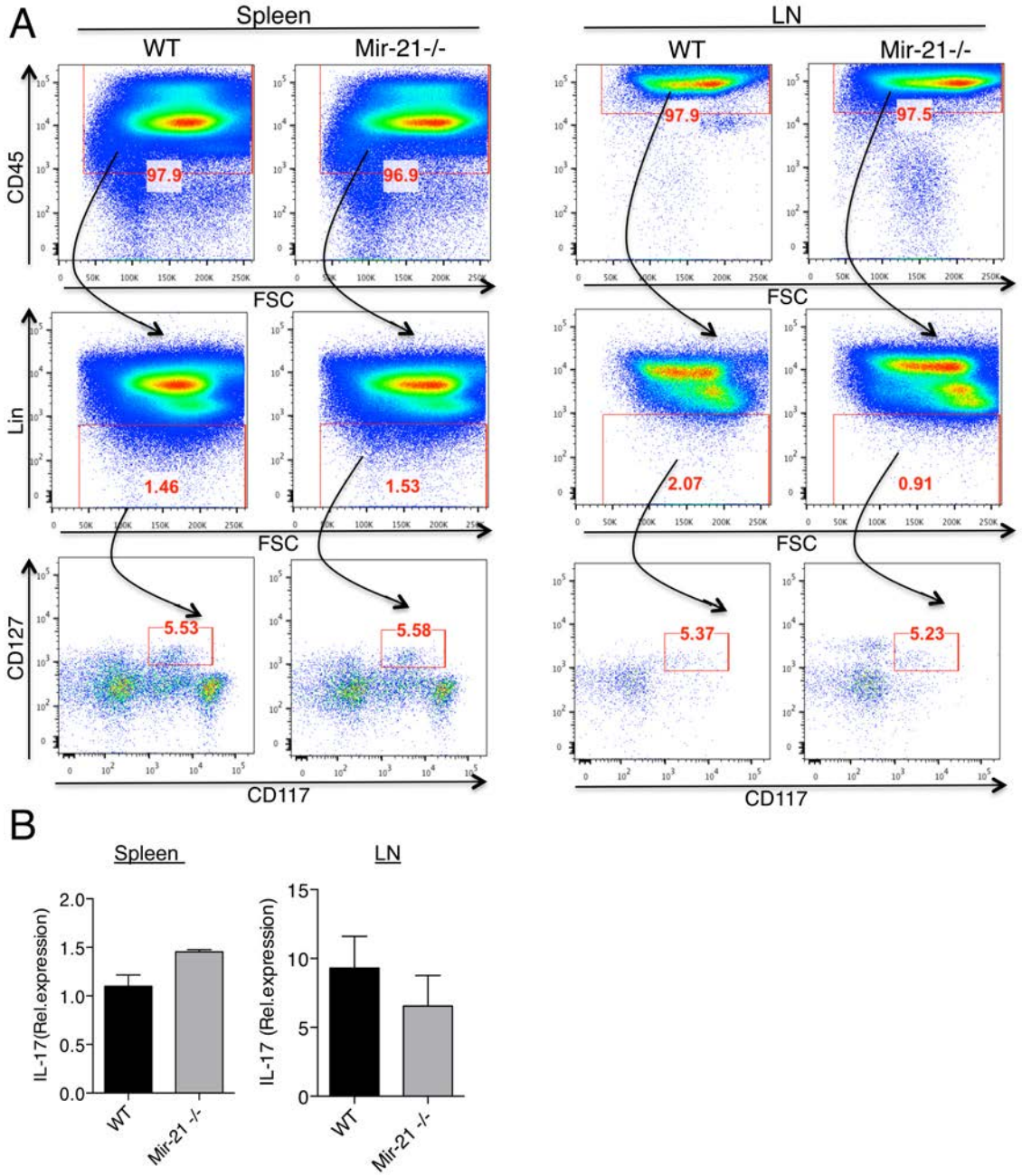

Supplemental Figure 9. **Unaltered innate lymphoid cells (ILCs) in Mir-21$^{-/-}$ mice. (A)** Flow cytometry analysis of innate lymphoid cells (ILCs) in spleen and LN of MOG_{35-55}-immunized WT and Mir-21$^{-/-}$ mice. ILCs are defined as CD45^{+} Lin^{-} (CD3^{-}, Ly6C/G^{-}, B220^{-}, CD11b^{-}, and CD11C^{-}) CD127^{+} CD117^{+} cells. (**B**) Quantitative RT-PCR analysis of IL-17 expression in sorted CD127^{+} CD117^{+} ILCs from WT and Mir-21$^{-/-}$ mice. Data are from two independent experiments.

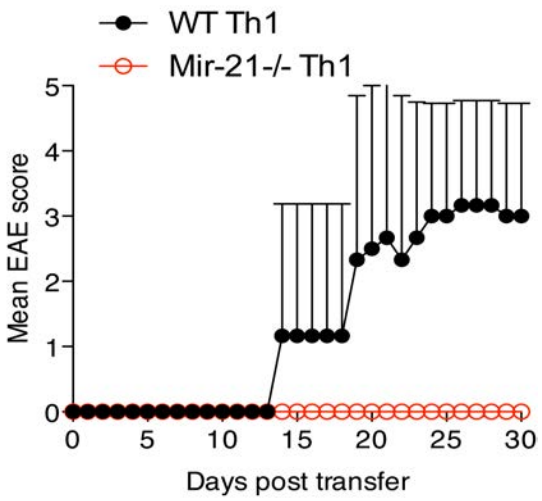

Supplemental Figure 10. Mir-21$^{-/-}$ Th1 cells fail to induce EAE. WT and Mir-21$^{-/-}$ mice were immunized with MOG_{35-55} peptide emulsified in CFA. At 10 days post MOG immunization, mice were sacrificed and $CD4^+$ T cells from spleen and LN were cultured for 5 days with MOG peptide (50 μg/ml) in the presence of IL-12 (20 ng/ml) before injection into WT recipients ($2x10^7$ cells/mouse). Recipients were injected with PT on the day of T cell transfer and again two days later. Clinical signs of EAE were monitored daily. Data are representative of two independent experiments.

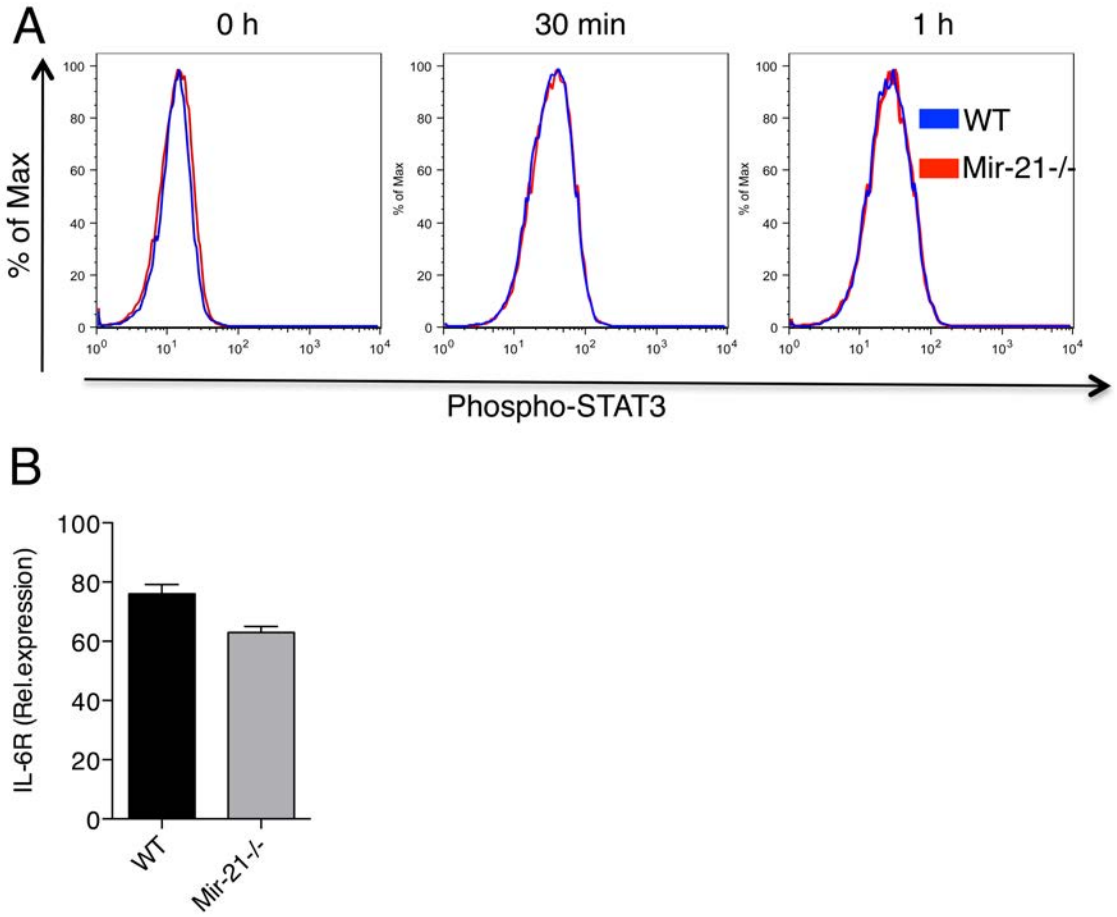

Supplemental Figure 11. Unaltered IL-6R and IL-6-induced STAT3 phosphorylation in Mir-21$^{-/-}$ CD4^{+} T cells. (A) Flow cytometry analysis of IL-6-induced STAT3 phosphorylation in CD4^{+} T cells from WT and Mir-21$^{-/-}$ mice. (**B**) The mRNA expression of IL-6R was analyzed by quantitative RT-PCR. Data are from two independent experiments. Error bars, mean ± SEM. *p<0.05, **p<0.01, ***p<0.001, unpaired Student's *t* test.

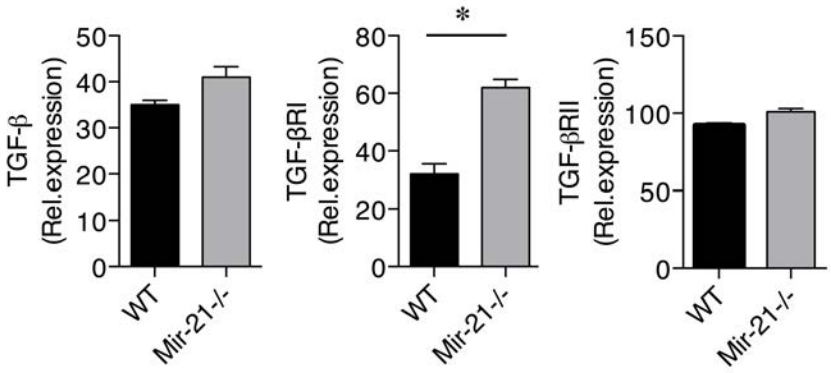

Supplemental Figure 12. TGF-β and TGF-βR expression is normal in Mir-21$^{-/-}$ CD4^{+} T cells. Quantitative RT-PCR analysis of TGF-β and TGF-βR expression in naïve CD4^{+} T cells from WT and Mir-21$^{-/-}$ mice. Data are from two independent experiments. Error bars, mean ± SEM. *p<0.05, **p<0.01, ***p<0.001, unpaired Student's *t* test.

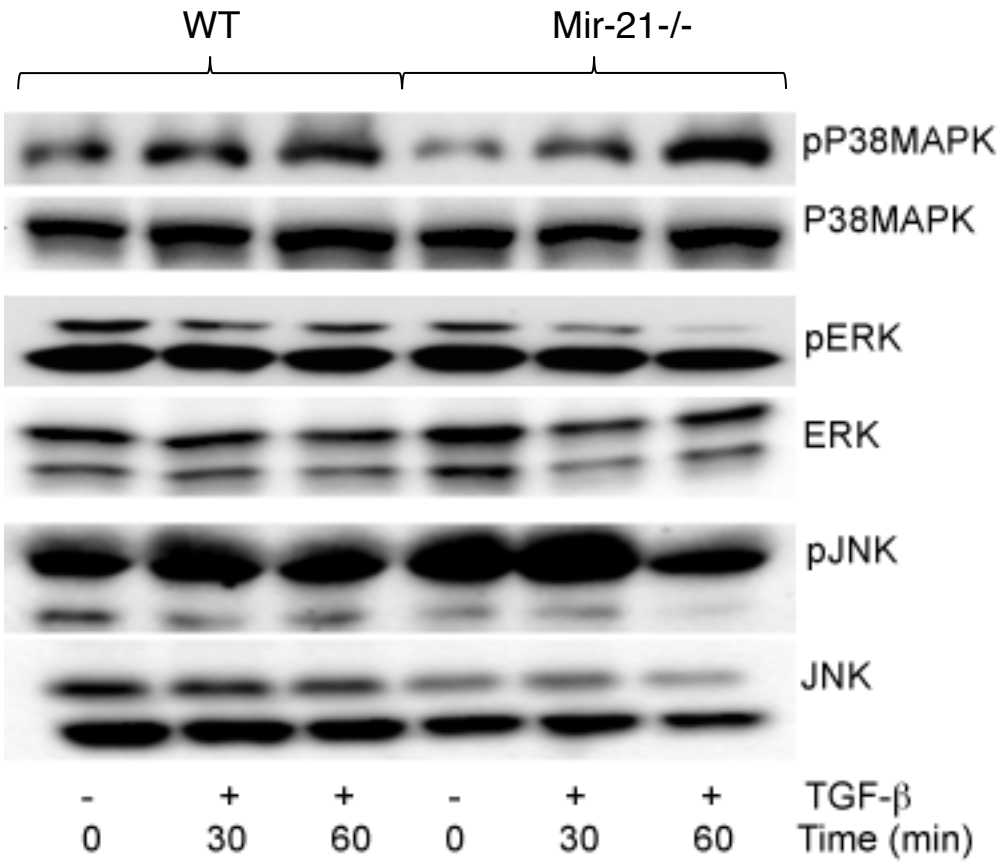

Supplemental Figure 13. TGF-β-induced non-Smad signaling pathway is normal in Mir-21$^{-/-}$ T cells. CD4^{+} T cells from WT and Mir-21$^{-/-}$ mice were stimulated for 24 hours with plate-bound anti-CD3 and anti-CD28 antibodies (2μg/ml). After 12 hours of resting, cells were stimulated with TGF-β (2 μg/mL) for the indicated times. Phosphorylated and total P38MAPK, ERK, and JNK proteins were detected in Western blot assays of cell lysates. Data are from two independent experiments.